International Journal of Pharmaceutics: X 10 (2025) 100432

Contents lists available at ScienceDirect

International Journal of Pharmaceutics: X

journal homepage: www.sciencedirect.com/journal/international-journal-of-pharmaceutics-x

Inhalative polyclonal immunoglobulin G for the prevention of respiratory infections: A comprehensive *in vitro* assessment

Rebecca Rittersberger [a,b], Caroline Covini [c], Shruthi Kalgudde [d], Pramod Kumar [d], Franziska Voß [e], Janik Martin [a,b], Franziska Magdalena Deuter [a], Gabriel Koslowski [a], Annabelle Dabbars [a], Sophia Salcher [a], Marion Blayac [d], Jürgen Römisch [c], Andrej Murányi [c], Jonas Knoch [f], Ali Önder Yildirim [d,g], Thomas M. Conlon [d], Otmar Schmid [d], Sven Hammerschmidt [e], Katharina Schindowski [a,*]

[a] *Institute of Applied Biotechnology, Biberach University of Applied Science, Hubertus Liebrecht Strasse 35-39, 88400 Biberach, Germany*
[b] *Faculty of Natural Science, University of Ulm, Albert-Einstein-Allee 11, 89081 Ulm, Germany*
[c] *Octapharma Pharmazeutika Produktionsgesellschaft mbH, Oberlaaerstrasse 235, 1100 Vienna, Austria*
[d] *Institute of Lung Health and Immunity (LHI), Helmholtz Munich, Comprehensive Pneumology Center (CPC-M), Member of the German Center for Lung Research (DZL), Ingolstädter Landstraße 1, 85764 Neuherberg, Germany*
[e] *Department of Molecular Genetics and Infection Biology, Interfaculty Institute for Ge- netics and Functional Genomics, Center for Functional Genomics of Microbes, University of Greifswald, Greifswald, Felix-Hausdorff-Str. 8, 17487 Greifswald, Germany*
[f] *PARI Pharma GmbH, Moosstrasse 3, 82319 Starnberg, Germany*
[g] *Institute of Experimental Pneumology, Ludwig-Maximilians University Munich, Marchioninistr. 15, 81377 München, Germany*

ARTICLE INFO

Keywords:
Protein formulation
Biopharmaceutics
Vibrating mesh nebulizer
IgG
Toxicity
FcRn
Quality

ABSTRACT

Inhalation therapy represents a promising strategy for the delivery of biopharmaceuticals for the local treatment of respiratory diseases. Purified polyclonal serum immunoglobulin G (IgG), also known as IVIg products, exhibit a solid reactivity against common viral and bacterial antigens. However, IVIg are usually delivered intravenously or subcutaneously, thus, not at the sites where most infections originate. Accordingly, a respiratory mucosal delivery of IVIg may have the potential to prevent infections at the mucosal barrier. To evaluate the feasibility and efficacy of inhalable IVIg for the prevention and therapy of respiratory infections, this study examined nebulization and its impact on protein quality, as well as potential effects on *in vitro* cytotoxicity and immunogenicity. IVIg were formulated with either 0, 200, or 400 µg/mL of polysorbate 80 (PS80). Formulation with polysorbate 80 resulted in less IgG aggregation during nebulization and thereby reduced *in vitro* immunogenicity. Further, the transepithelial transport was analyzed using two different airway epithelial models, with no effects observed due to either nebulization or formulation. Finally, the efficacy of formulated aerosolized IVIg against *Streptococcus pneumoniae* TIGR4 model bacteria was assessed. The results demonstrated a dose-dependent binding of relevant *S. pneumoniae* antigens and efficient dose-dependent opsonophagocytosis of *S. pneumoniae*.

Abbreviations: ADCC, antibody-dependent cellular cytotoxicity; ADCP, antibody-dependent cellular phagocytosis; ADE, antibody-dependent enhancement; ALI, air-liquid interface; ANOVA, analysis of variance; CFU, colony-forming units; CI, confidence interval; CMC, critical micelle concentration; COVID-19, corona virus disease 2019; Ct, cycle threshold; DLS, Dynamic light scattering; DMSO, dimethyl sulfoxide; Fab, antigen-binding fraction; FBS, fetal bovine serum; FcRn, neonatal Fc receptor; FDA, food and drug administration; HBSS, Hank''s buffered salt solution; Hprt1, Hypoxanthine phosphoribosyl transferase 1; IC50, half-maximal inhibitory concentration; IgG, immunoglobulin G; IL-1β, Interleukin 1β; IL-6, Interleukin 6; IVIg, intravenously applied immunoglobulin; LDH, lactate dehydrogenase; LPS, lipopolysaccharide; MCC, mucociliary clearance; mean diff, mean differences; MEM, Minimal essential medium; MFI, mean fluorescence intensity; MOI, multiplicity of infection; MPPD, Multiple Path Particle Dosimetry Model; OBB, opsonization buffer B; OD600, optical density at 600 nm; PBS, phosphate buffered saline pH 7.4; PS80, polysorbate 80; RSV, human respiratory syncytial virus; RT-qPCR, real time quantitative polymerase chain reaction; SARS-CoV-2, severe acute respiratory syndrome corona virus type 2; SCIg, subcutaneously applied immunoglobulin; SD, standard deviation; SE-HPLC, Size exclusion high-performance liquid chromatography; *S. pneumoniae*, *Streptococcus pneumoniae*; TEER, trans-epithelial electrical resistance; THY, Todd – Hewitt-Yeast broth; TMPC, Tracheal mucosal primary cells; TNF-α, Tumor necrosis factor α; USP, United States Pharmacopeia; VMD, volume median diameter; WHO, world health organization; WST1, Water soluble tetrazolium salt..

* Corresponding author.
E-mail address: schindowski@hochschule-bc.de (K. Schindowski).

https://doi.org/10.1016/j.ijpx.2025.100432
Received 29 March 2025; Received in revised form 12 October 2025; Accepted 27 October 2025
Available online 30 October 2025

In conclusion, this study indicated the promising potential of inhaled polyclonal IVIg as a**n effective** therapy against respiratory infections.

1. Introduction

The corona virus disease 2019 (COVID-19) pandemic has underscored that lower respiratory infectious diseases remain a significant threat in the 21st century. Pneumonia, caused by bacteria such as *Streptococcus pneumoniae* (*S. pneumoniae*; the pneumococcus) or *Haemophilus influenzae*, and viruses like influenza or the *human respiratory syncytial virus* (*RSV*), was the fourth leading cause of death worldwide even before the emergence of severe acute respiratory syndrome corona virus type 2 (SARS-CoV-2) (official website of world health organization WHO: https://www.who.int/news-room/fact-sheets/detail/the-top-10-causes-of-death; 03.01.2024 22:32; (The top 10 causes of death, 2025). Children, the elderly, and immunocompromised individuals are particularly vulnerable, whereas most immunocompetent adults without severe pre-existing conditions can often manage these infections without intensive medical intervention. For instance, infections with *S. pneumoniae* are responsible for 1.6 million deaths annually, causing not only pneumonia but also sepsis, meningitis, and otitis media (Song et al., 2013). Colonization typically occurs asymptomatically, with invasive disease primarily affecting high-risk groups (Steurer et al., 2022).

Treating respiratory infections can be challenging. For viral infections, effective treatments are often limited by (i) a lack of proven therapies, (ii) a narrow therapeutic window post-infection, and (iii) potential development of resistance to antiviral drugs (Batool et al., 2023; Gatt et al., 2023). Bacterial infections, on the other hand, face the growing challenge of antibiotic resistance, driving research and the development of new therapeutics (Cella et al., 2023). Therefore, protecting high-risk groups from severe respiratory infections is a more strategic approach than treating acute severe conditions. Although vaccination remains the most effective preventive measure, vaccines are not available for all pathogens, and immunocompromised individuals may not develop sufficient immunity (Marcotte and Hammarström, 2015; Verwey and Madhi, 2023). Therefore, passive immunotherapy with polyclonal immunoglobulin G (IgG) products from healthy donors may offer a valuable strategy to prevent and reduce severe respiratory infections in immunocompromised and immunosuppressed patients (Borte et al., 2017). Currently, such IgG products are administered intravenously (IV; IVIg) or subcutaneously (SC; SCIg) (Mersich et al., 2017), but for respiratory infections, inhalation of such products could improve the delivery to the site of action with a direct impact on mucosal immunity (Greeley, 2017; Henning et al., 2008; Ladel et al., 2018; Sato and Kiyono, 2012; Tsai et al., 2023). Additionally, inhalation, which is suitable for outpatients, is cost-effective for healthcare services and potentially requires less medication compared to systemic administration (Cahn et al., 2023; McElroy et al., 2013).

Although polyclonal IgGs or anti-infective monoclonal IgGs show promise for infection prevention as therapeutic agents, aerosolization of proteins, particularly IgG, remains a challenging task (Parray et al., 2021). Aerosolization exposes the proteins to the air-liquid interface (ALI) and may induce thermal and mechanical stress (Bodier-Montagutelli et al., 2018; Röhm et al., 2017). These factors cannot only decrease the proteins' efficacy, but also increase their immunogenic potential (Ahmadi et al., 2015; Moussa et al., 2016; Ratanji et al., 2014; Vultaggio et al., 2012; Wang et al., 2012). Vibrating mesh nebulizers induce less thermal and mechanical stress compared to jet, ultrasonic-, or soft mist inhalers, potentially preserving IgG stability (Bodier-Montagutelli et al., 2018; Hertel et al., 2015; Röhm et al., 2017). Apart from the choice of the aerosolization device, formulation with excipients such as polysorbates can help to maintain protein integrity during aerosolization (Bodier-Montagutelli et al., 2018; Hertel et al., 2015; Röhm et al., 2017; Stützle et al., 2015).

This study aims to evaluate the feasibility of an inhalable polyclonal IVIg product for the prevention and therapy of pneumococcal infections. Using a vibrating mesh nebulizer, we characterized the aerodynamic properties and stability of nebulized IgG. IgG aggregation was successfully reduced with a suitable formulation of polysorbate 80 (PS80). The formulated nebulized IgG was then tested for potential toxicity and immunogenicity as predictor for drug safety. IgG uptake and transport were evaluated in airway mucosa models. Finally, *in vitro* efficacy against *S. pneumoniae* was determined by binding of the IgGs to the pathogen, neutralization, and opsonophagocytosis.

2. Materials and methods

2.1. Material

Panzyga® (Octapharma, Austria) was used as IVIg either in its original formulation (100 mg/ mL polyclonal human IgG in 230 mM glycine buffer) or in glycine buffer containing polysorbate 80 (PS80) as indicated. Most chemicals and media were purchased from Thermo Fisher (Darmstadt, Germany), Carl Roth (Karlsruhe, Germany) or Sigma-Aldrich/Merck (Taufkirchen, Germany) unless otherwise indicated. Reactivity of Panzyga® against 22 *S. pneumoniae* serotypes was determined in a clinical diagnostic lab as previously reported (Mersich et al., 2017).

2.2. Nebulizer and characterization of aerosol and nebulized IVIg

For all investigations, an eFlow® Technology vibrating-mesh nebulizer (PARI Pharma GmbH, Starnberg, Germany) equipped with a customized mesh was used. Up to 8 mL of the solution were nebulized. The nebulizer output rate was evaluated by measuring the time until more than 98 % of product was fully nebulized or until the device stops. The output rate is presented as volume per time (mL/min).

Aerosol droplets were collected by condensation into polypropylene (PP) tubes for further investigations. Aerosol droplet size (volume median diameter, VMD) was measured with a Spraytec™ (Malvern Panalytical Ltd., Malvern, UK) device equipped with an inhalation cell at a 90° angle (constant aspiration with 15 L/min) airflow at room temperature. The recording time was 2 min.

The lung deposited aerosol dose can be estimated from the product of inhaled dose and fractional aerosol deposition in the lung. The delivered (inhalable) IgG dose in patients was determined by nebulization into a breathing simulator (BRS 200i, Copley, Nottingham, UK) operated with filtered ambient air (relative humidity 40–60 %) and a polypropylene filter (Copley, Nottingham, UK) for complete IgG aerosol removal at room temperature (20–25 °C). An adult breathing pattern according to European Pharmacopeia 2.9.44, with a tidal volume of 500 mL, 15 breaths per minute, and an inhalation-exhalation ratio of 1:1 was used for the nebulization of 2 mL IgG solution (European Pharmacopeia, 2022; Jauernig et al., 2008). To calculate the delivered dose, the filter was rinsed with glycine buffer for 1 h on an orbital shaker after nebulization and the IgG concentration was determined by UV spectrometry (NanoPhotometer NP80, Implen, Germany). Subsequently, the MPPD (Multiple-Path Particle Dosimetry) computational aerosol lung deposition model was applied (Miller et al., 2016) to determine the aerosol deposition fraction in the bronchial region of the lung considering i) the same breathing pattern as mentioned above, ii) the empirically determined performance parameters of the eFlow® nebulizer for IVIg (VMD, output rate) iii) oral aerosol inhalation, and iv) the symmetric lung morphology (Yeh and Schum, 1980). The bronchial dose was selected,

since both cell types selected for toxicity testing are models of the big conducting lower airways. The bronchially deposited IgG dose could then be calculated from the product of nebulized IVIg mass, the delivered dose fraction and the bronchially deposited aerosol fraction.

For post nebulization integrity testing, aerosol droplets were collected by condensation into sterile 15 mL polypropylene (PP) test tubes. The collected solution was stored at 2–8 °C until analysis, alongside with a non-nebulized Panzyga® control sample. The concentration of IgG solutions before and after nebulization was determined using a Nanophotometer (NanoPhotometer NP80, Implen, Germany) at 280 nm to evaluate any changes during the nebulization process.

SE-HPLC (1260 HPLC system, Agilent, Santa Clara, United States) with a TSK G3000 SW 10 µm column (Tosoh Bioscience LLC, Tokyo, Japan) was used to quantify molecular size distribution of monomers, dimers, polymers, and fragments according to the European Pharmacopeia monograph 8.00918, general methods 2.2.29 and 2.2.46 (European Pharmacopeia, 11th Ed., English: 11.0–11.2, 2022) after nebulization. The samples were filtered through a polyethersulfone 0.22 µm syringe filter (Merck Millipore, Darmstadt Germany) into glass vials. Results were expressed as changes in monomer and dimers and/or polymer content relative to the non-nebulized control.

Z-average diameter (intensity-weighted mean diameter) was determined with dynamic light scattering (DLS; Malvern Zetasizer Nano-ZS (Malvern Instruments Ltd., Malvern, UK). Samples were measured undiluted. Subvisible particulates (1–100 µm) were determined with flow imaging (FlowCam, Yokogawa Fluid Imaging Technologies, Scarborough, USA) and light obscuration (PAMAS GmbH, Rutesheim, Germany). FlowCam results were evaluated after the removal of air bubbles and are expressed as the total number of particles (≥ 2 µm), particles larger than 25 µm (≥ 25 µm), and particles larger than 10 µm (≥10 µm). The percentage increase of particles was calculated after nebulization relative to the non-nebulized control.

2.3. Cell culture, cytotoxicity and immunogenicity assays

Tracheal mucosal primary cells (TMPC) were isolated from pigs and cultured as described previously (Martin et al., 2024). Briefly, the mucosa was used within 1–2 h *post mortem*. The tissue samples were disinfected with Octenisept® (Schülke & Mayr GmbH, Norderstedt, Germany), digested with pronase (Sigma-Aldrich, Taufkirchen, Germany) and purified with debris removal solution (Miltenyi Biotec, Bergisch Gladbach, Germany). The cells were directly seeded into rat tail collagen type I (Primacyte, Schwerin, Germany) coated 24-well membrane inserts (1 µm pore size, 0.336 cm^2, Greiner Bio-One, Kremsmünster, Austria) with 10^5 cells/insert. After 24 h, the cells were lifted to ALI conditions by removing the apical medium and differentiated for 21 days. RPMI 2650 (ATCC no. CCL-30), derived from a nasal squamous mucosa cancer, were cultivated on above-mentioned inserts (Kreft et al., 2015).

Calu-3 (ATCC no. HTB-55), a human bronchial adenocarcinoma cell line was seeded into 12-well transwell inserts (0.4 µm pore size, 1.12 cm^2, Corning, New York, USA) with 10^5 cells/cm^2 and cultivated for 5–6 days under submerged conditions in MEM GlutaMAX supplemented with 1 % NEAA, 1 % Penicillin/Streptomycin (all from: Thermo Fisher) and 10 % FBS (Sigma-Aldrich) (Zhu et al., 2010). 24 h after air-lift, 50 µL of IVIg either undiluted (100 mg/mL for 4.46 mg/cm^2 IgG) or diluted with glycine buffer were added apically. For transport studies, medium without FBS was used.

Transepithelial electrical resistance (TEER) of the cell barriers was determined with an EVOM3 device with chopstick electrodes (World Precision Instruments, Sarasota, USA). The resistance of a blank membrane insert without cells was subtracted and the resulting value was multiplied by the growth area of the membrane inserts (here: 1.12 or 0.336 cm^2 depending on cell type) as previously described (Ladel et al., 2019; Martin et al., 2024). TMPCs and Calu-3 were used for permeability studies only when the TEER value was above 500 Ω cm^2.

Metabolic activity as measure of cell viability was analyzed with Alamar Blue according to the manufacturer's instructions with MEM without phenol red (both from Thermo Fisher) as negative control and 50 % dimethyl sulfoxide (DMSO, Carl Roth, Karlsruhe, Germany) as cytotoxic positive control (Zachari et al., 2014). 100 µL samples were added apically and 260 µL of MEM without phenol red were applied basolaterally. After 24 h the samples were removed and replaced by 100 µL of a 1:10 dilution of Alamar Blue in MEM for 5 h at 37 °C. The fluorescence was measured with 530 nm excitation and 590 nm emission. According to ISO 10993-5 guideline, substances are defined as "non-cytotoxic" if the viability ≥70 % (Grosu, 2022). Water soluble tetrazolium salt (WST1; Roche, Basel, Switzerland) and lactate dehydrogenase (LDH; Roche, Basel, Switzerland) as viability and cytotoxicity assays, respectively, were performed on Calu-3 cells according to manufacturer's instructions.

Murine dendritic DC2.4 cells were plated overnight at 0.25 × 10^6 cells/well in 24-well plates with a surface area of 1.9 cm^2/well (Lu et al., 2024). DC2.4 cells were exposed to a dose of 4.46 mg IVIg/cm^2 either formulated with 0, 200 or 400 µg/mL PS80. Lipopolysaccharide (LPS; 100 ng/mL) was used as positive control and PS80-containing glycine buffer as negative control. RNA was extracted (RNeasy Plus Mini Kit, Qiagen, Venlo, Netherlands), cDNA synthetized (High-Capacity RNA-to-cDNA, Applied Biosystems, Waltham, USA) and expression analyzed using PowerUp SYBR Green Master Mix (Applied Biosystems™, Waltham, USA) in real-time quantitative polymerase chain reaction (RT-qPCR). Primer sequences for murine interleukin-6 (IL6; gene *Il6*), interleukin-1β (IL-1β; gene *Il1B*), and tumor necrosis factor-alpha (TNF-α; gene *Tnf-α*), and the house-keeping gene Hypoxanthine phosphoribosyl transferase 1 (gene: *Hprt1*) are indicated in Table 1. Relative expression was calculated relative to Hprt1 as $2^{-\Delta ct}$ (cycle threshold), and fold changes compared to vehicle control samples were expressed as $2^{-\Delta\Delta ct}$ values.

2.4. Transepithelial transport of IVIg in different formulations

Apical to basolateral transport studies were performed in the ALICE Cloud system (Vitrocell, Waldkirch, Germany) with the stainless-steel extension plates (see Supplementary materials and methods, Fig. M1; specifically designed and adapted for us by Rolf Pfäffle from Beiter GmbH & Co KG, Sigmaringendorf, Germany). In brief, 200 µL of 20 mg/mL IVIg containing either, 200 or 400 µg/mL PS80 (Carl Roth) were nebulized with the eFlow® and deposited on membrane inserts with TMPC differentiated at ALI for 21 days (Fig. M1C and D). The deposited volume per well was determined beforehand (see Supplementary materials and methods) as 0.73 ± 0.34 µL for 20 mg/mL IVIg with 200 µg/mL PS80 (total applied dose 43.45 ± 20.24 µg/cm^2 IgG and 434.52 ± 202.38 ng/cm^2 PS80) and 0.66 ± 0.40 µL (total applied dose 39.29 ± 23.81 µg/cm^2 IgG and 785.71 ± 476.19 ng/cm^2 PS80) for 20 mg/mL IVIg with 400 µg/mL PS80. Samples were taken after 0.5 up to 48 h from the basolateral side. IgG was quantified with a sandwich ELISA using two polyclonal human Fc region-specific antibodies (both from Sigma-Aldrich, capture: #I2136; 1: 7500 dilution; detection: #A0170; 1:50,000 dilution). Due to the demonstrated impairment of quality, the native IVIg formulation was excluded in this experimental set-up.

2.5. Evaluation of in vitro efficacy against Streptococcus pneumoniae strain TIGR4

Binding of nebulized IVIg to 55 protein antigens of *S. pneumoniae* was determined with a fluorescent xMAP bead-based multiplex immunassay (Luminex Licensed Technology Group, Austin, Texas, USA) on Flexmap 3D system as described previously (He et al., 2024; Meyer et al., 2020; Schmidt et al., 2017; Seinen et al., 2021). Briefly, antigens were conjugated to xMAP microspheres and incubated with diluted IVIg samples. Beads incubated with PBS (phosphate buffered saline pH 7.4) were used as blanks. Data processing with the xMAP pipeline included filtering,

Table 1
Primer sequences used for the immunogenicity assay.

Marker for	mRNA target	Forward Primer (5′-3′)	Reverse Primer (5′-3′)
House-keeping	*Hprt1*	AGCTACTGTAATGATCAGTCAACG	AGAGGTCCTTTTCACCAGCA
cytokines	*Il1B*	GCCCATCCTCACTCAT	AGGCCACAGGTTGTCG
	Il6	GTTCTCTGGGAAATCGTGGA	TGTACTCCAGGTAGCTATGG
	Tnf-α	CACCACGCTCTTCTGTCT	GGCTACAGGCTTGTCACT

blank substraction, normalization and calculation of the mean fluorescence intensity (MFI) (Meyer et al., 2020). The response values were calculated as the product of the half-maximal dilution factor and its corresponding MFI.

Binding of IVIg to the surface of pneumococci was evaluated by flow cytometry (FACSCalibur, Becton Dickinson, Franklin Lakes, USA) equipped with FlowJo 10.8.1 software (FlowJo LLC, Ashland, USA). TIGR4, a serotype 4 *S. pneumoniae* strain, was inoculated in THY medium with 2 % Yeast Extract (Carl Roth) with an OD_{600} of 0.08 and cultivated in a water bath at 37 °C to an OD_{600} of 0.35–0.4. TIGR4 bacteria were incubated with IVIg, washed, and stained with anti-hFc-AF488 (#2040–30, Southern Biotech, Birmingham, USA).

To determine a potential neutralizing activity of IVIg, TIGR4 were cultivated to OD_{600} 0.2, aliquoted and IVIg added to a final concentration of 1 mg/mL. Glycine buffer was used as negative control. The OD_{600} was measured every 30 min for a total of 3 h.

The Fc-dependent effector function of IVIg was evaluated by an opsonophagocytosis assay using murine J774A.1 macrophages. IVIg diluted in HBSS with Ca/Mg^{2+} (Thermo Fisher) with 5 % FBS (Capricorn Scientific, Ebsdorfergrund, Germany) were incubated with a TIGR4 suspension (100,000 colony forming units (CFU)/mL). Polyclonal anti-pneumococcal IgG, purified from rabbit serum was used as the positive control and glycine buffer as negative control (Heß et al., 2017). After 30 min incubation, the opsonized bacteria were transferred to the J774A.1 macrophages with a final multiplicity of infection (MOI) of 400:1 ($\sim 1.2 \times 10^6$ macrophages/cm^2, ~ 2941 CFU/cm^2 and 5.76 mg IgG/cm^2 for highest IgG dose) and incubated. The CFU of the viable TIGR4 cells was quantified by plating them on blood agar plates (Thermo Fisher).

2.6. Statistical analysis, illustrations and declaration of generative AI and AI-assisted technologies in the writing process

All results are presented as mean ± standard deviation (SD) unless otherwise stated. Graphs were created and statistical evaluation was performed using GraphPad Prism 9 and 10 software (Boston, USA). Biostatistical tests are indicated below. Technical replicates are indicated as "n" and biological replicates as "N" in table/ figure descriptions. Illustrations were created under license with biorender.com. For English language correction and conciseness, the language model ChatGPT (GPT-4) from openai.com was used.

3. Results and discussion

In order to evaluate the *in vitro* feasibility of inhalable IVIg for the prevention and therapy of *S. pneumoniae* infections, the aerosolization and its impact on protein quality, cytotoxicity and immunogenicity were determined first. Next, the transepithelial transport was analyzed in two airway epithelial models and finally the efficacy against *S. pneumoniae* of aerosolized IVIg was assessed.

3.1. Addition of PS80 effectively prevents nebulization-induced IgG aggregation

As demonstrated previously, the stability of nebulized protein aerosols is critical for the biopharmaceutical's quality, and their distribution in the airways depends on their aerodynamic properties (Ahmadi et al., 2015; Darquenne, 2020; Moussa et al., 2016; Ou et al., 2020; Podczeck, 1999). Since PS80 has been shown to prevent aggregation during nebulization (Mayor et al., 2022), PS80 as additive for nebulized IVIg was investigated by different methods (Fig. 1A) for the occurrence of subvisible (1–100 µm) and submicron (0.1–1 µm) particles. Nebulization had no clear effect on the formation of subvisible particles (Supplementary Fig. 1). Therefore, it was not too surprising that PS80 had no significant effect on subvisible particles determined by flow imaging (Supplementary Fig. 1A) or by light obscuration (Supplementary Fig. 1B).

In contrast, nebulization increased the occurrence of submicron particles in IVIg without PS80 (white bar in Fig. 1B), decreased the number of IgG monomers (−0.35 ± 0.13 %; white bar in Fig. 1C) and increased the occurrence of IgG polymers (+0.3 %; white bar in Fig. 1D). The addition of PS80 effectively prevented submicron aggregation in nebulized samples in a dose-dependent manner (blue bars in Fig. 1B-D). Measuring undiluted samples, the *Z*-average of the original IVIg product without PS80 increased due to nebulization by 0.18 ± 0.02 nm, which is an increase of 1–2 % compared to the IgG monomer diameter of 10–15 nm (Tan et al., 2008). 200 and 400 µg/mL PS80 significantly reduced the Z-Average of nebulized IVIg by 0.06 ± 0.03 nm (**$p \leq 0.01$) and 0.04 ± 0.08 nm (**p ≤ 0.01), respectively (blue bars in Fig. 1B). The same observations could be made when samples were diluted 1:5 in 0.9 % NaCl before measurement (data not shown). Additionally, the PDI values can be found in Supplementary Table S2. Analysis of the IgG mono- and dimer content by SE-HPLC implicated non-significant tendency towards increased levels with PS80 as additive (200 µg/mL PS80: −0.28 ± 0.096 %, 400 µg/mL PS80: −0.17 ± 0.15 %; blue bars in Fig. 1C) while a significant reduction of IgG polymers was observed (200 µg/mL PS80: 0.15 ± 0.06 %, **p ≤ 0.01; 400 µg/mL PS80: 0.1 %, ***$p \leq 0.001$; blue bars in Fig. 1D).

This analysis demonstrated the effectiveness of PS80 as excipient in preserving IgG quality during aerosolization consistent with prior findings (Röhm et al., 2017). Aerosolization exposes proteins to air-liquid interfaces, risking denaturation, aggregation, and reduced efficacy if formulations are not optimized for inhalation (Bodier-Montagutelli et al., 2020). Aggregated proteins may also trigger unwanted immunogenicity (Ahmadi et al., 2015; Mettelman et al., 2022; Moussa et al., 2016; Sécher et al., 2022). Polysorbates, widely used in parenteral and respiratory protein drug formulations, stabilize proteins by displacing them from interfaces (here: at surface of aerosols) when used above their critical micelle concentration, preventing intermolecular interactions, and act as molecular chaperones in refolding partially denatured proteins (Arsiccio and Pisano, 2018; Matthews et al., 2020; Mayor et al., 2022; Tao et al., 2023; Wuchner et al., 2022).

A higher variability in subvisible particle formation was observed in formulations without PS80, which failed to achieve statistical significance compared to those with PS80. Aggregates may still form or dissolve post-application to mucosal surfaces (Narhi et al., 2012). On the other hand, aggregate formation follows in general a nucleation growth mechanism where monomers attach to existing aggregation cores, causing aggregates to grow over time (Auer et al., 2007). Future studies may explore the long-term stability of different formulations under conditions that simulate the conditions of the respiratory mucosa.

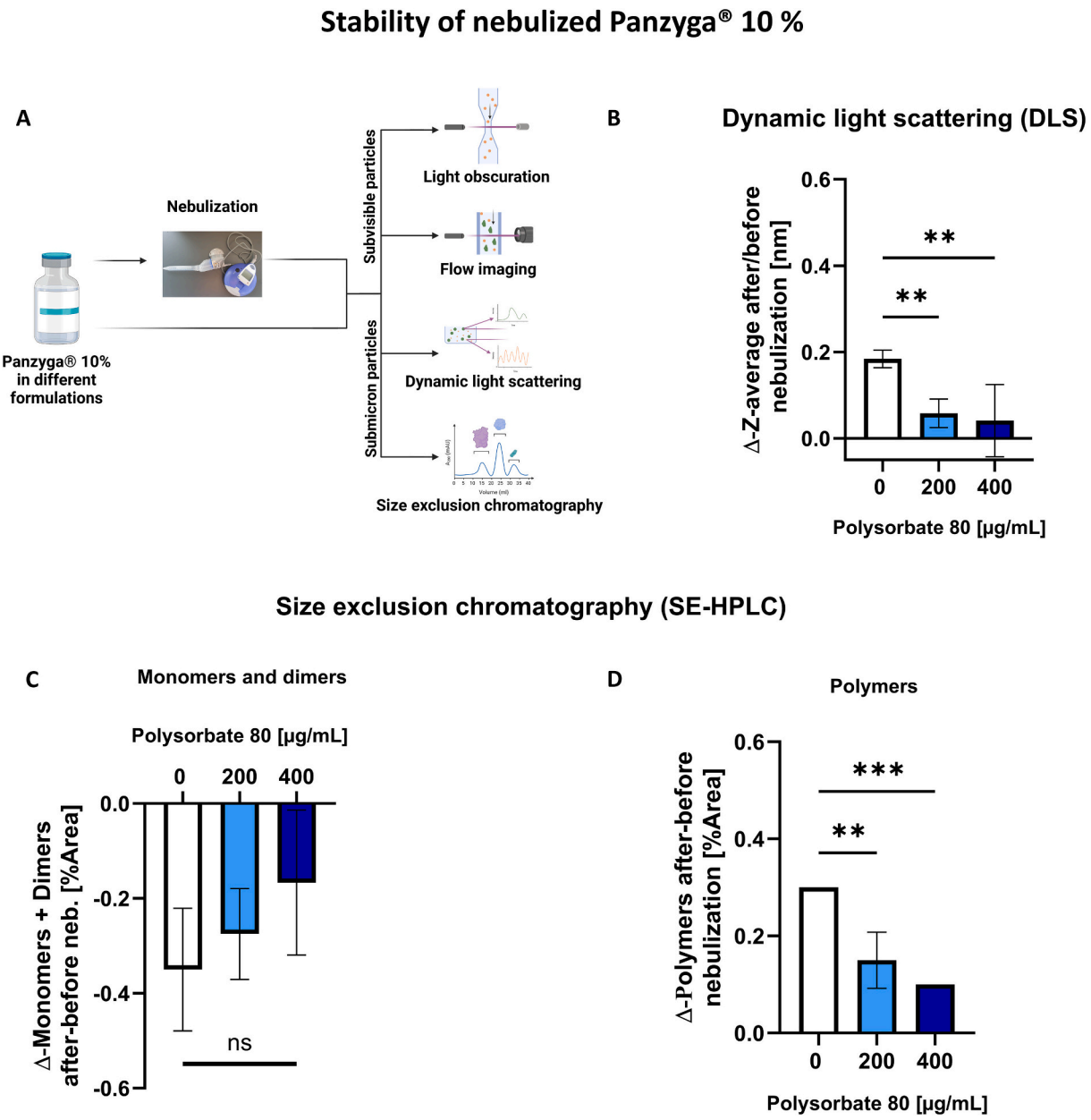

Fig. 1. Particle and aggregates analysis of IVIg (Panzyga®) in different formulations with PS80 after nebulization with eFlow® nebulizer. A) Particle analysis methods utilized in this study. Unnebulized and nebulized samples were compared in flow imaging and light obscuration for subvisible particles (see supplementary fig. S1) and SE-HPLC and DLS for submicron particles. Created under license with biorender.com B) DLS: Change in particle size/ diameter after nebulization in different formulations with PS80 in comparison to unnebulized IVIg product as control, expressed as Δ-*Z*-average (undiluted IVIg, $n = 3$). C) Monomer and dimer decrease analysis *via* SE-HPLC, presented as % of area (n = 3). D) Polymer increase analysis *via* SE-HPLC, presented as % of area (n = 3). Values are shown as mean ± SD. n = nebulization of independent samples. Ordinary one-way analysis of variance (ANOVA); not significant (ns) $p > 0.05$, *$p \leq 0.05$, **$p \leq 0.01$, ***$p \leq 0.001$, ****$p \leq 0.0001$.

3.2. *Characterization of IVIg aerosol nebulized with the eFlow® nebulizer*

The performance of aerosol-generating devices and the characteristics of the aerosol are key factors impacting drug safety, efficacy, cost-effectiveness, and patient compliance (Ahmadi et al., 2015; Arunthari et al., 2012; Moussa et al., 2016). Aerodynamic properties of aerosols, alongside factors like breathing pattern, airway morphology, and gas properties, are essential for predicting drug distribution within the airways (Bui et al., 2020; Chen et al., 2021; Darquenne, 2020; Ou et al., 2020; Pilou, 2020; Podczeck, 1999). Therefore, IVIg was either tested in its marketed form without PS80 or formulated with 200 or 400 µg/mL PS80. A dose of 200 mg IgG of each formulation was then nebulized and the time recorded when the nebulization was completed. This so-called liquid output rate of the nebulizer is a critical parameter for patient therapy adherence, as it directly correlates inversely with the required nebulization or inhalation time (Hogan et al., 2015). The nebulization of all formulations demonstrated that a dose of 200 mg IgG was nebulized within roughly 4 min (Table 2). The addition of PS80 to Panzyga® IVIg had no significant effect on output rates (~0.5 mL/min or ~ 50 mg IgG/min; $p > 0.05$, see Table 2) or the nebulized amount of liquid (at least 98 %, data not shown). The measured output rate aligns with Panzyga®'s viscosity of 3.35 ± 0.15 mPa·s for 100 mg/mL (Mersich et al., 2017) and was higher than previously reported data of an IVIg of 40 mg/mL and lower viscosity of 1.34 mPa × s with a KTMED mesh nebulizers (output rate of ~0.2–0.3 mL/min) (Chang et al., 2023). However, here determined output rate was still lower than the maximum described output

Table 2
Aerosol characteristics and inhalable dose of differently formulated IVIg nebulized with an eFlow® nebulizer loaded with 2 mL of 100 mg/mL IVIg. "n = "indicates the nebulization of independent samples.

IVIg 100 mg/mL IgG	original formulation without PS80	Addition Of		One-way ANOVA
		200 µg/mL PS80	400 µg/mL PS80	
IgG dose nebulized	200 mg	200 mg	200 mg	
Output rate [mL/mg]	0.52 ± 0.06 (*n* = 4)	0.47 ± 0.06 (n = 4)	0.50 ± 0.04 (*n* = 3)	$p > 0.05$ (ns)
Delivered (inhalable) dose fraction [%]	62.11 ± 7.88 (n = 4)	54.22 ± 5.33 (n = 4)	65.00 ± 2.89 (n = 4)	$p > 0.05$ (ns)
VMD [µm]	2.21 ± 0.04 (*n* = 6)	2.35 ± 0.07 (n = 3)	2.31 ± 0.03 (n = 3)	$p \leq 0.01$ (**) for 0 *vs.* 200 µg/mL PS80, otherwise $p > 0.05$ (ns)

rate of the eFlow® with 1 mL/min (Ari, 2014), likely due to the high viscosity (Beck-Broichsitter et al., 2014; Chang et al., 2023). This finding highlights the impact of viscosity on nebulization efficiency, which is critical because prolonged nebulization times can increase agitation, interface exposure, and temperature changes, potentially affecting protein stability (Hertel et al., 2015).

A higher nebulizer output rate does not guarantee a higher inhalable dose, as the dose delivered to the mouthpiece may not increase proportionally (Hong et al., 2023). Using a breathing simulator and an adult breathing pattern according to the European Pharmacopeia, the delivered dose of 2 mL Panzyga® nebulized with different PS80 concentrations was assessed (European Pharmacopeia, 11th Ed., English: 11.0–11.2, 2022). The customized eFlow® nebulizer is a continuously operating device with a valved aerosol chamber, in which the aerosol produced during the exhalation phase is collected and made available for inhalation at the onset of the following inhalation. The device delivered ~54–65 % of the initial dose regardless of PS80 concentration (Table 2). Delivered doses vary significantly with device type and patient breathing patterns, even at constant output rates. Differences have been observed for simulated breathing patterns of adults' and children's as well as between of breathing-impaired (*e.g.* asthma) and healthy patients rates (Hong et al., 2023). Breath-activated nebulizers could enhance efficiency by minimizing drug loss and reducing patient discomfort (Arunthari et al., 2012). Only a fraction of the inhaled dose deposits in the lung, with deposition influenced by aerosol size, respiratory profile, lung morphology, age, sex, and disease type (Zhang et al., 2024).

Therefore, the aerosol size was assessed for different PS80 formulations as indicated in Table 2. A statistically significant increase in the average VMD was observed for IVIg with 200 µg/mL PS80 in comparison to IVIg without PS80 (2.21 ± 0.04 µm for native IVIg and 2.35 ± 0.07 µm for IVIg with 200 µg/mL PS80, ** $p \leq 0.01$). However, such small variations in droplet size (<10 %) are not likely to have any effect on the biological effects of IgG. Generally, a size of 2–3 µm is optimal for deposition in the alveolar region (Borghardt et al., 2018). Previous preclinical studies with similar aerosol parameters have shown *in vivo* efficacy of inhaled IgG (Vonarburg et al., 2019). Investigating aerosol deposition in the upper airways could be valuable for preventive anti-infective therapy with polyclonal IgG, as infections often originate there before spreading to the lung. The upper airways, rich in immunocompetent cells, play a critical role in early immune defense (Greeley, 2017; Haley, 2003; Tschernig and Pabst, 2000).

3.3. Even high doses of aerosolized IVIg do not show any cytotoxic effects

Preclinical dose estimations and toxicology studies are crucial for regulatory approval (Hacker, 2009). Therefore, different cytotoxicity assays were performed with IgG doses chosen to match or exceed the maximum clinically expected localized bronchial dose of up to 2 mg/cm^2 IVIg for the eFlow® aerosol parameters determined above (output rate: 0.5 mL/min, IgG concentration: 100 mg/mL, inhaled dose fraction: 60 %, VMD: 2.3 µm, IVIg aerosol density: 1 g/cm^3). Consequently, for a 15 min inhalation session the resulting inhalable dose for a non-impaired breathing adult is 451 mg (= 15 min · 0.5 mL/min · 100 mg/mL · 60 %), which corresponds to a tissue-normalized bronchially deposited dose of 0.0056 mg/cm^2 (= 0.13 · 451 mg / 10,000 cm^2, the latter representing the bronchial epithelial area (ICRP, 1994)) leveraging the bronchial aerosol dose fraction of 0.13 obtained with the well-established MPPD computational aerosol-lung deposition model (Miller et al., 2016). Thus, the *in vitro* applied doses of up to 4.46 and 29.76 mg/cm^2 depending on cell type (see below) are at least 1000-fold larger than the clinically expected average dose. Even, if we consider as a worst-case condition an up to 350-fold dose enhancement factor at very confined local hot spots due to aerosol impaction near the carina of airway bifurcations (Balashazy et al., 2003) the local IgG dose in patients does not exceed 2.0 mg/cm^2 and is therefore well below the *in vitro* doses tested here for toxicity. The cellular models employed in this study included both established epithelial cell lines, commonly used to represent different regions of the respiratory tract, as well as primary cells isolated from the conducting airways (trachea). These ALI-differentiated models have been extensively characterized in recent studies (Martin et al., 2024). Initial toxicity testing of unnebulized IVIg with 29.76 mg/cm^2 under submerged conditions on TMPC and RPMI 2650 cells showed no cytotoxic effects, regardless of PS80 concentration (Fig. 2A). The assay performed determines the redox potential of the mitochondria of viable cells. The results were normalized to the medium control. According to ISO 10993-5, samples with viability ≤70 % are considered as toxic. TMPC viability exceeded even 100 %, while RPMI 2650 showed a statistically insignificant minor viability decrease for IVIg with 400 µg/mL PS80, still above the ISO 10993-5 threshold. Viability exceeding 100 % may be due to differences in batches, cell number after differentiation, or in mitochondrial activity (Silva et al., 2023; Yoon et al., 2000).

Subsequent tests with nebulized IVIg formulations confirmed these findings (Fig. 2B). While TMPC again showed viability values over 100 % (****$p \leq 0.0001$), RPMI 2650 samples showed no significant differences across formulations, with viabilities around 100 %. Full data is provided in Supplementary table S3.

To evaluate potential cytotoxicity in a bronchial model, Calu-3 cells were exposed to 4.46 mg/cm^2 of nebulized IVIg with 0, 200, or 400 µg/mL PS80 (equivalent to 0, 8.93, or 17.86 µg/cm^2 PS80). Cytotoxic effects were assessed 72 h post-exposure using WST1 for metabolic activity, LDH release for cytotoxicity, and TEER for barrier integrity (data not shown). Similar to RPMI 2650 cells, no significant changes were observed in WST1 or LDH assays compared to untreated cells ($p > 0.05$). TEER measurements also showed no significant decreases relative to initial values ($p > 0.05$), with unnebulized samples ranging from 602.2 ± 46.99 Ω° cm^2 (0 h, no PS80) to 724.8 ± 96.91 Ω° cm^2 (72 h, 400 µg/mL PS80) and nebulized samples ranging from 593.1 ± 65.49 Ω° cm^2 (0 h, no PS80) to 734.6 ± 70.35 Ω° cm^2 (72 h, 400 µg/mL PS80). These findings indicate no cytotoxic effects of nebulized IVIg *in vitro*.

It is well known that not only immunoglobulin but also PS80 can cause toxic effects (Lindenberg et al., 2019; Metz et al., 2020). The reported *in vitro* IC50 for PS80 calculated as delivered dose per area, ranges from ~606–6061 µg/cm^2 (Metz et al., 2020). FDA approved concentrations in other products are consistent with the dose range used here (Metz et al., 2020).

Antibodies are generally safe in toxicity tests, and any observed toxicity is antigen- and/or target-related (Brennan et al., 2010; Hanson et al., 2006). For nebulized IgG, the primary concern is immunogenicity, particularly due to protein aggregation during nebulization (Sécher et al., 2022).

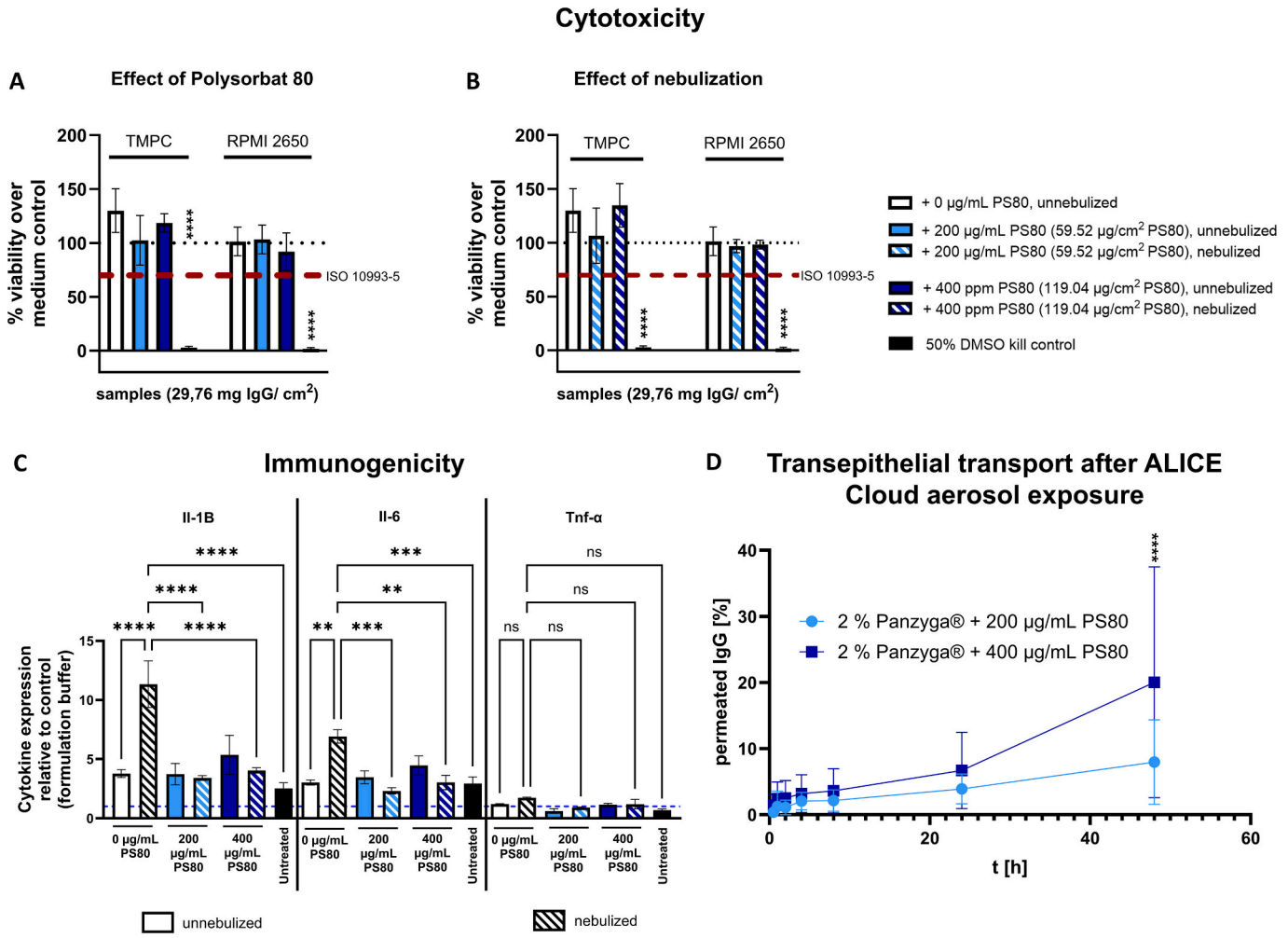

Fig. 2. Cytotoxicity, immunogenicity and transepithelial transport of (nebulized) IVIg with different PS80 concentrations: A) Comparison of a potential toxic effect of IVIg containing 0; 200; or 400 µg/mL PS80 on TMPC, RPMI 2650 cells, respectively. N = independent experiments, n = membrane inserts per sample. TMPC: $n = 20$, $N = 2$–4. RPMI 2650: n = 20–25, $N = 3$–5. B) Comparison of a potential toxic effect of nebulized IVIg containing 0; 200; or 400 µg/mL PS80 *vs.* the originally formulated unnebulized IVIg product on TMPC or RPMI 2650. N = independent experiments, n = membrane inserts per sample. TMPC: n = 20, N = 2–4. RPMI 2650; $n = 15$–25, N = 2–5. Blue dotted line represents 100 % viability, normalized with samples exposed to MEM medium control. Red dotted line represents 70 % viability threshold according to ISO 10993-5. C) Potential immunogenic effect of IVIg in different formulations before (open boxes) or after nebulization (hashed boxes) on dendritic DC2.4 cells. Cells were stimulated with IVIg with no PS80, or with addition of PS80 (200/ 400 µg/mL). Post stimulation, proinflammatory cytokine expression, Il-6, Il-1β and Tnf-α levels were measured after 6 h *via* quantitative RT-PCR and 2-ΔΔCt values were calculated. n = 2, $N = 2$. N = biological replicates and n = technical replicates. Values are shown as mean ± SD. Ordinary one-way ANOVA; $p > 0.05$, not significant (ns), *$p < 0.05$; **$p < 0.01$; ***$p < 0.001$, ****$p < 0.0001$. D) Transepithelial permeability of nebulized IVIg (20 mg/mL) containing 200; or 400 µg/mL PS80 on TMPC over 48 h. $n = 14$/ 28, N = 2. N = independent aerosol exposure experiments *via* the ALICE Cloud system, n = membrane inserts per sample. Values are shown as mean ± SD. Two - way ANOVA; $p > 0.05$, not significant (ns), *$p < 0.05$; **$p < 0.01$; ***$p < 0.001$, ****$p < 0.0001$. (For interpretation of the references to colour in this figure legend, the reader is referred to the web version of this article.)

3.4. Addition of PS80 decreases immunogenicity of nebulized IVIg

Biopharmaceuticals of inferior quality (*i.e.* denatured and/or aggregated) have the potential to induce immune responses that can vary in extent, potentially leading to loss of efficacy or even anaphylactic reactions (Ahmadi et al., 2015; Moussa et al., 2016; Wang et al., 2012). Even though no significant increase in aggregate formation was observed in PS80-formulated IVIg, an *in vitro* immunogenicity assay was performed to exclude any potential safety concerns. The dendritic cell line DC2.4 was exposed to unnebulized and nebulized IVIg formulated either with 0, 200, or 400 µg/mL PS80 for 6 and 24 h and the proinflammatory cytokines IL-6, IL-1β, and TNF-α were quantified *via* RT-qPCR. The results were compared to untreated DC2.4 as control. The results are depicted in Fig. 2C. In concordance with the occurrence of submicron particles (Fig. 1B-D), nebulized IVIg without PS80 significantly increased the expression of two out of three cytokines compared to untreated cells (****$p \leq 0.0001$ for *Il-1B* and ***$p \leq 0.001$ for Il-6, ns > 0.05 for *Tnf-α*), its unnebulized counterpart (****p ≤ 0.0001 for *Il1-B*, **$p \leq 0.01$ for *Il-6,* ns > 0.05 for *Tnf-α*), and the unnebulized and nebulized samples containing PS80 after 6 h (****p ≤ 0.0001 for *Il1-B*, **/***p ≤ 0.001/ 0.0001 for *Il-6,* ns > 0.05 for *Tnf-α*). With the addition of PS80, the fold change of cytokine expression after nebulization could be lowered significantly (*e.g.* from 11.3 ± 1.97 (*Il-1B*, nebulized IVIg without PS80) to 3.4 ± 0.21 (*Il-1B*, ****p ≤ 0.0001) for nebulized IVIg with 200 µg/mL PS80 and to 4.0 ± 0.23 (*Il-1B*, ****p ≤ 0.0001) for nebulized IVIg with 400 µg/mL PS80. Cytokine expression levels between unnebulized and nebulized samples of IVIg with PS80 showed no significant differences ($p > 0.05$). No significant differences between any samples were detected after 24 h (data not shown, $p > 0.05$). Given the small sample size, we would like to point out that this study should be regarded as exploratory. The ANOVA yielded an overall significant effect ($F(21,22) = 26.09$, $p < 0.0001$, $\eta^2 = 0.9614$). Detailed data,

including mean differences and 95 % confidence intervals, are provided in Supplementary Table S4.

In conclusion, formulations are crucial for inhaled protein delivery and while guidelines for parenteral products (*e.g.*, United States Pharmacopeia 788) limit the number of particles per container, they do not apply to inhaled formulations (Ibrahim et al., 2023). Subvisible (1–100 μm) and submicron (0.1–1 μm) particles have been both implicated in immune activation (Joubert et al., 2012; Kijanka et al., 2018; Telikepalli et al., 2015; Thorlaksen et al., 2023). For instance, mice inhaling aggregated proteins experienced adverse immune events (Sécher et al., 2022) and even non-aggregated inhaled insulin increased anti-insulin antibody levels in mice due to *in vivo* aggregate formation (Lasagna-Reeves et al., 2010). Non-aggregated proteins delivered to the respiratory tract may aggregate upon deposition on tissue surfaces (Matthews et al., 2020). Different aggregate characteristics such as size or shape may influence immunogenicity (Baranov et al., 2020; Thorlaksen et al., 2023). Protein modifications, including misfolding or oxidation, may expose immunogenic epitopes, however the impact of other changes, like deamidation, remains underexplored (Hermeling et al., 2004; Moussa et al., 2016; Thorlaksen et al., 2023). These findings underscore the importance of stabilizing formulations to minimize protein aggregation and ensure safety and efficacy. This aspect is of particular relevance, as the respiratory mucosa is not simply a static barrier but rather a highly dynamic and adaptive tissue capable of mounting context-dependent responses, for example during infection or injury (Davis and Wypych, 2022; Hewitt and Lloyd, 2021; Mettelman et al., 2022). Antigen-presenting cells (APCs), including dendritic cells and macrophages, play a central role in this process by sensing and internalizing xenobiotics either within the lamina propria, the alveolar interstitium, or directly at the epithelial interface (Blanco-Melo et al., 2020; Hiemstra et al., 2015; Mettelman et al., 2022). Their activation can initiate a cascade of immune events, such as the recruitment of additional effector cells from the circulation or the priming of B and T lymphocytes within lymphoid tissues (Mettelman et al., 2022). Consequently, investigating the effects of nebulized biopharmaceuticals on APCs is crucial for determining whether a given product has the potential to elicit airway immune responses.

3.5. PS80 may influence transepithelial transport of IVIg in airway models

Effective passive immunization *via* inhalation requires IgG to interact with both pathogens and resident immune cells, which are primarily located in the *lamina propria* beneath the epithelial barrier (Sato and Kiyono, 2012). To investigate whether nebulization or PS80 affects transepithelial transport, a study using the TMPC airway epithelial model was conducted, applying 43.45 ± 20.24 μg/cm^2 IgG for 20 mg/mL IVIg with 200 μg/mL PS80 and 39.29 ± 23.81 μg/cm2 IgG for 20 mg/mL IVIg with 400 μg/mL PS80. The two formulations differed significantly only at the final sampling time point (48 h), with 7.95 ± 6.40 % of the applied IgG dose transported across the epithelial layer for 200 μg/mL PS80, compared to 20.03 ± 17.45 % for 400 μg/mL PS80 (****$p \leq 0.0001$; Fig. 2D). The large standard deviations may be attributed to variability in the small deposited aerosol volumes across wells, compounded by error propagation during percentage calculations. Notably, the effect of PS80 was not observed when higher IgG doses were applied *via* pipetting—29.76 mg/cm^2 on TMPCs (data not shown) or 0.37 mg/cm^2 on Calu-3 cells ($p > 0.05$; Supplementary Fig. S5).The conducting airways are predominantly lined by a pseudostratified epithelium composed of multiple cell types, including ciliated cells, goblet cells, club cells, and basal cells (Martin et al., 2024). This epithelial layer contributes to host defense through two major mechanisms: (i) mucociliary clearance (MCC), and (ii) barrier integrity maintained by tight and adherens junctions between neighbouring cells. Together, these functions form the first line of unspecific protection against xenobiotics, whether pathogenic microorganisms or, as in this study, administered drugs (Martin et al., 2024). Recent work has shown that *in vitro* airway epithelial models such as TMPC and Calu-3 cells can recapitulate key epithelial features to varying extents following differentiation under ALI conditions (Martin et al., 2024). These models exhibit properties such as the formation of a tight epithelial barrier and the secretion of mucins and additional secretory proteins. Further, robust neonatale Fc receptor (FcRn) levels relevant for IgG recycling and transcytosis were observed in airway tissue as well as the cellular models (Martin et al., 2024). This receptor-mediated transport likely accounts for the absence of a dose-dependent PS80 effect at high IgG concentrations, despite PS80's established permeability-enhancing properties for small molecules and peptides (Azmin et al., 1982; Gao et al., 2019; Ruan et al., 2012). Considering the complexity of the aerosol exposure procedure in the ALICE Cloud system, it would be of interest for future studies to examine whether receptor-mediated transepithelial transport exhibits IgG dose dependency in the presence of excipients such as PS80.

3.6. In vitro efficacy of nebulized IVIg against S. pneumoniae

3.6.1. Binding of nebulized IVIg to individual pneumococcal antigens and whole bacterial cells

Respiratory infections can be caused by various pathogens, including *S. pneumoniae*, which has over 100 serotypes and is a common cause of pneumonia, particularly in immunocompromised or comorbid patients (Blasi, 2004; Borchardt and Rolston, 2012). To confirm that Panzyga® IVIg binds to *S. pneumoniae* model strain TIGR4 effectively, an xMAP bead assay was conducted with 55 pneumococcal protein antigens (Fig. 3A and Supplementary Table S6 for detailed antigen information). The xMAP bead assay (Fig. 3B) revealed that response values varied significantly between antigens and formulations (Fig. 3A). The highest responses were observed for Pneumococcal histidine triad protein D (PhtD) and the peptidoglycan hydrolase PcsB, while the beta-galactosidase SP_0060, the surface protein Dimorphic invasion-involved A DiiA/ SP_1992, Thioredoxin reductase TrxB, and zinc ion-binding lipoprotein AdcAII showed the lowest responses. For some samples, like the major autolysin (LytA) and streptococcal lipoprotein rotamase A (SlrA), no response value could be calculated as the curve fitting failed. A two-way analysis of variance (ANOVA) revealed significant differences between formulations, with PS80-containing, unnebulized samples showing higher response values compared to native, unnebulized IVIg. However, nebulized samples did not show significant response differences between PS80 concentrations (200 *vs.* 400 μg/mL, $p > 0.05$). The nebulization of the PS80-containing samples generally reduced the response, particularly at 400 μg/mL (****$p < 0.0001$). In contrast, nebulization of the native formulation had no significant effect on the response. PS80 primarily interacts with the antigen-binding fraction (Fab) region of antibodies, affecting their tertiary structure, rather than the Fc region (Garidel et al., 2009; Singh et al., 2017). Singh et al. attributed these findings to the lower thermodynamic stability of the Fab region compared to the Fc domain (Singh et al., 2017). In addition to stabilization through interface replacement, which is particularly critical during the aerosolization process, polysorbates have also been described as so-called *chemical chaperones* (Agarkhed et al., 2013). By binding to hydrophobic patches of partially unfolded proteins, they can increase the energy barrier to further unfolding and promote correct refolding (Agarkhed et al., 2013). Within the Fab region, such refolding activity may have contributed to maintaining antigen-binding functionality; however, additional experiments, beyond the scope of this study, would be required to confirm this. Notably, nebulization reduced the effect of PS80, resulting in response levels comparable to those of native, unnebulized IVIg. The secondary F(ab)$_2$ fragment used in this study is a polyclonal product that, according to the manufacturer, "reacts with the Fc portion of the human IgG heavy chain but not with the Fab portion of human IgG. No antibody was detected against human IgM or IgA, or against non-immunoglobulin serum proteins" (dianova Int., 2025). However, no information is

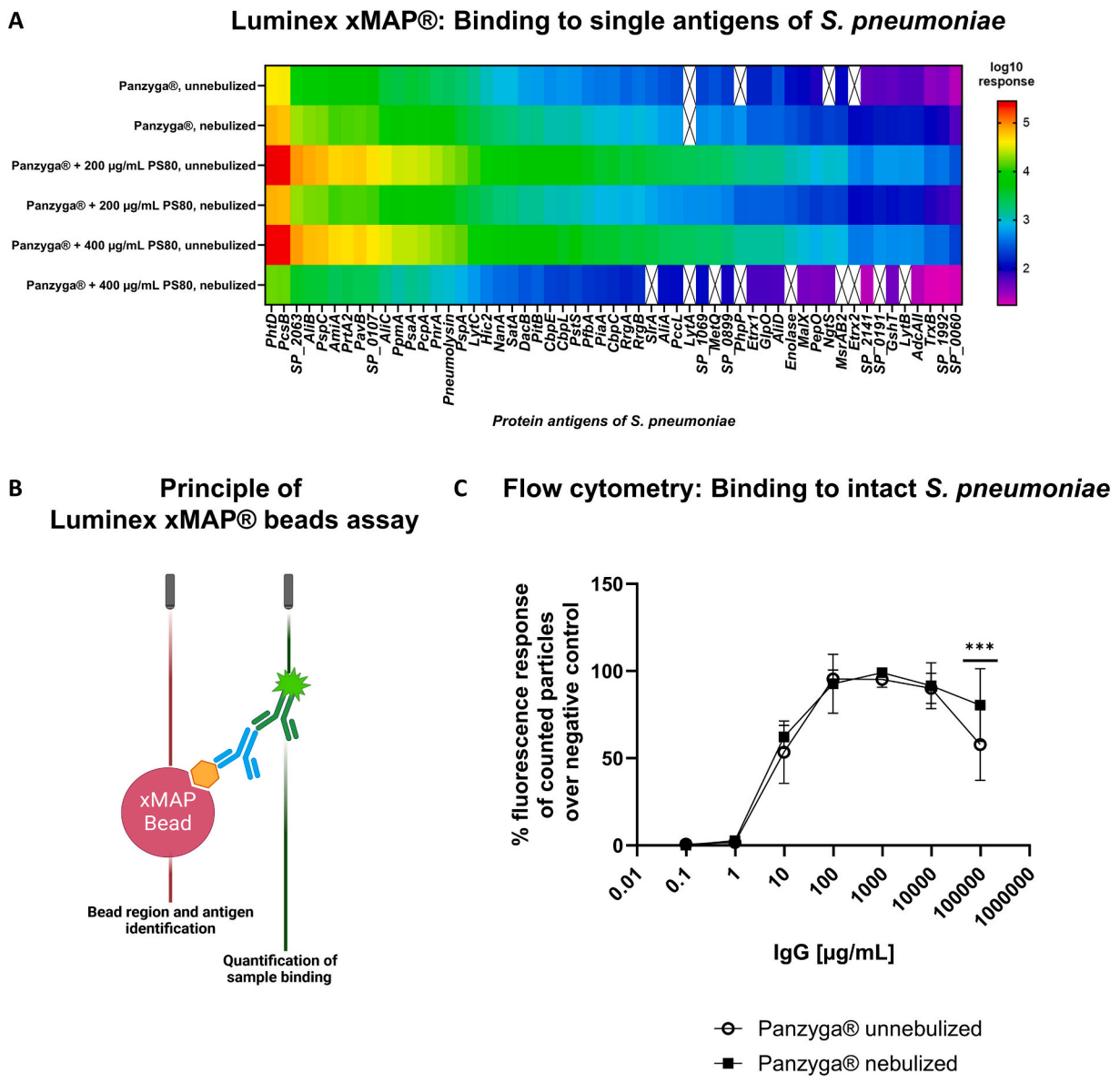

Fig. 3. Binding of nebulized IVIg (Panzyga®) to individual pneumococcal antigens (xMAP assay), and to whole bacterial cells. (A) Heat map of the logarithmic response values of (un-)nebulized IVIg samples to 55 protein antigens of *S. pneumoniae*. The response values were calculated based on seven serial dilutions of the indicated samples following saturation curve modelling. White boxes indicate missing values, where data point fitting failed or was rejected. Information on tested antigens, their abbreviations, full name and functions is provided in Supplementary Table S6. Overall two-way ANOVA between the different samples revealed the following differences: $^{****}p < 0.0001$ for unnebulized IVIg without PS80 compared to unnebulized IVIg with 200 µg/mL PS80; $^{***}p < 0.001$ for unnebulized IVIg without PS80 compared to unnebulized IVIg with 400 µg/mL PS80, $p > 0.05$ (ns) for unnebulized IVIg with 200 µg/mL PS80 compared to unnebulized IVIg with 400 µg/mL PS80. Nebulized samples showed no significant differences between the different concentrations of PS80 ($p > 0.05$). Samples with added PS80 showed significant differences between nebulized and unnebulized samples ($^{***}p < 0.001$ for IVIg with 200 µg/mL PS80 and $^{****}p < 0.0001$ for IVIg 10 % with 400 µg/mL PS80). Nebulization of the native formulation had no significant effect on the response to the antigens ($p > 0.05$). As a standard procedure, each (nebulized) sample was measured in 7-fold dilution series with a single measurement for each dilution step to cover a wide range of IgG responses ($N = 1$, $n = 1$ per IgG concentration, 7-fold dilution series per (nebulized) sample) This process has been repeatedly published in investigations of antibody titers in *e.g.* patient sera or sputa (He et al., 2024; Meyer et al., 2020; Schmidt et al., 2017; Seinen et al., 2021). B) Schematic principle of the Luminex xMAP beads assay: The beads are internally labeled and discriminable with different compositions of fluorescent dyes excited at 525 nm. After IVIg incubation, the antigen-specific IgG quantification is conducted by binding of a R-phycoerythrin-labeled secondary antibody excited at 635 nm. Created with biorender.com C) Dose-dependent binding study of (un-)nebulized IVIg to whole *S. pneumoniae* TIGR4 *via* flow cytometry. Illustrated are the percentages of fluorescent positive bacteria relative to the negative control (fluorophore coupled secondary antibody only) in dependency of the IgG concentration. Nebulized IVIg contained 400 µg/mL PS80. N = independent experiments, $n = 4$ samples (wells) measured twice by flow cytometry. $n = 8$, $N = 2$ Values are shown as mean ± SD. Two-way ANOVA; $P > 0.05$, not significant (ns); $^{*}p < 0.05$; $^{**}p < 0.01$; $^{***}p < 0.001$; $^{****}p < 0.0001$.

provided regarding potential subclass specificity within human IgG, which are present in IVIg preparations (Mersich et al., 2017). Consequently, differences in binding affinity between IgG subclasses cannot be ruled out.

After confirming binding of nebulized IVIg to individual antigens, flow cytometry was used to evaluate dose-dependent binding of IVIg to whole *S. pneumoniae* TIGR4 cells. Given the minimal differences observed with 200 or 400 µg/mL PS80 in previous tests, only IVIg with 400 µg/mL PS80 was included in this experiment. Fig. 3C demonstrates that the human polyclonal IVIg binds to TIGR4 in a dose-dependent

manner and a saturation in binding at concentrations ≥98 μg/mL. No significant differences were observed between unnebulized IVIg without PS80 and nebulized IVIg with 400 μg/mL PS80 ($p > 0.05$), except for the highest concentration of 98 mg/mL IgG (***$p < 0.001$). It is important to note that at this high concentration, the bacteria pellet could not be properly formed by centrifugation, leading to more error-prone processing of these samples. In conclusion, these results confirm that *S. pneumoniae* TIGR4 is a suitable model for testing inhaled IVIg efficacy.

3.6.2. Addition of IVIg does not impair growth of S. pneumoniae TIGR4

Antibody-dependent cellular phagocytosis (ADCP) and neutralization by prevention of colonization are particularly relevant against bacterial infections, although complement activation plays also an essential role (Fig. 4A) (Bebbington and Yarranton, 2008; Müller-Loennies et al., 2007; Yoong, 2010). Binding of IVIg to key proteinaceous colonization factors such as PspC, PsaA (Elm et al., 2004; Kadioglu et al., 2008; Mitchell and Mitchell, 2010), PcsB, and Ami-AliA/AliB (critical for bacterial cell division and nutrient uptake) (Alcorlo et al., 2024; Bartual et al., 2014), as wells as to whole TIGR4 bacteria was observed. Therefore, the effect of 1 mg/mL nebulized IVIg on the growth of *S. pneumoniae* TIGR4 over 3 h was investigated. All samples reached the stationary phase (Fig. 4B), indicating no substantial effect on bacterial growth. It should be noted that minor differences between conditions were visible after 2 h, but all samples reached stationary phase, indicating no substantial effect on bacterial growth. Direct bactericidal activity of IgGs was observed against Borrelia (LaRocca et al., 2008). Despite the binding of IVIg to TIGR4, the polysaccharide capsule of *S. pneumoniae* can mask antigens, reducing IgG binding (Voß et al., 2018; Zangari et al., 2021). Further, IgG binding to an antigen does not necessarily compromise antigen functionality (Schieffelin et al., 2010). Lastly, it is important to note that Panzyga® comprises polyclonal IgGs targeting diverse pathogens and antigens (Mersich et al., 2017). Consequently, the concentration of IgG specific to individual antigens beneath the capsule might have been insufficient for effective bacterial growth inhibition at the tested ratio.

3.6.3. Nebulized IVIg mediates opsonophagocytosis of S. pneumoniae TIGR4

For effective defense against pathogens, the respiratory mucosa contains various immunocompetent cells such as macrophages and dendritic cells (APCs), collectively referred to as the mucosal-associated immune system that monitore the luminal mucosal surface for antigens (Sato and Kiyono, 2012). APCs are central to the initiation of mucosal immune responses, particularly in the context of IgG-mediated protection, which critically relies on interactions between IgG and Fc gamma receptors (FcγRs). Upon sensing and internalizing immune complexes, APC activation triggers a range of downstream immune processes, including the recruitment of additional immunocompetent cells from the circulation and the activation of B and T lymphocytes within lymphoid tissues (Blanco-Melo et al., 2020; Hiemstra et al., 2015; Mettelman et al., 2022). Hence, to bridge *in vitro* findings with subsequent preclinical *in vivo* studies, we conducted an opsonophagocytosis assay with *S. pneumoniae* TIGR4 and the murine macrophage cell line J774.A1 to assess the Fc-mediated phagocytosis of nebulized IVIg. Polyclonal anti-pneumococcal IgGs raised in rabbits (Heß et al., 2017) served as positive control, while negative controls included medium containing vehicle (230 mM glycine with 400 μg/mL PS80). Opsonophagocytosis was measured by CFU reduction on blood agar plates. IVIg doses ≥218 μg significantly decreased the CFU count with both unnebulized (**$p \leq 0.01$, compared to negative controls, represented by the orange dotted lines in Fig. 4C) and nebulized IVIg (*$p \leq 0.05$, compared to negative controls). No significant differences could be detected between unnebulized and nebulized IVIg ($p > 0.05$). At lower doses, no significant difference compared to negative control was observed. Calculation of IC50 values revealed 3832 μg/mL IgG for unnebulized IVIg and 4319 μg/mL IgG for the nebulized samples necessary to decrease CFU count by 50 %. These results indicate that high doses of IVIg are necessary to support ADCP of one specific pathogen like *S. pneumoniae*. In comparison, rabbit anti-pneumococcal IgG, isolated from hyperimmune serum containing high levels of antibodies specific to pneumococci (Heß et al., 2017), effectively reduced CFU counts even at lower doses (~12 μg, ****$p \leq 0.0001$, compared to negative controls, calculated IC50 140.7 μg/mL IgG). Notably, Panzyga® contains IgGs against a broad spectrum of pathogens, with anti-pneumococcal antibodies representing a small fraction. A titer of 552 ± 54 μg/mL against 22 different *S. pneumoniae* serotypes was assessed in this study for 7 batches tested comparable to previously reported 646 ± 126 μg/mL (Mersich et al., 2017). However, it should be noted that these values reflect the overall concentration against the multiple serotypes, and specific concentrations of IgG targeting serotype 4 are expected to be lower, although some cross-reactivity among serotypes has been reported (Nahm et al., 1997). Nonetheless, using the 646 μg/mL concentration allows for better comparison with the control rabbit hyperimmune serum, which demonstrated effective reduction down to approximately 12 μg IgG (~607 μg/mL), with CFU counts comparable to those of the highest IVIg samples. In general, the opsonization assay represents a biologically relevant *in vitro* method for assessing IgG-mediated antibacterial activity. However, translating the resulting *in vitro* dose–response relationship to *in vivo* or clinical contexts is challenging, as therapeutic efficacy depends not only on IgG concentration but also on macrophage abundance and bacterial burden (CFU). Under *in vitro* conditions, a design-of-experiment approach incorporating these three parameters could be applied. In patients, by contrast, local IgG levels, macrophage density, and bacterial load are expected to vary substantially depending on airway region, disease state or general health conditions and the timing of infection and IgG administration. These variations are further influenced by the lung's clearance mechanisms for both, IgG and bacteria. As a result, direct extrapolation of *in vitro* IgG opsonization data to clinical outcomes remains difficult.

4. Conclusion

This study highlights Panzyga®'s (IVIg's) potential as an inhaled preventive therapy for common respiratory infections. As antibiotic resistance and future pandemics become more pressing, preventative therapies are essential (Antimicrobial resistance, 2024; Williams et al., 2023). For patients with compromised immune systems, passive immunization with IVIg offers a promising alternative to active immunization, which may be ineffective for these groups (Borte et al., 2017; Marcotte and Hammarström, 2015). Inhaled IVIg offers a needle-free, home-administered option that delivers antibodies directly to the airways, potentially improving effectiveness in the early stages of infection (Cahn et al., 2023; Marcotte and Hammarström, 2015; Tsai et al., 2023; Vonarburg et al., 2019).

However, some aspects of IVIg delivery *via* inhalation require improvement or further investigation: higher concentrations of IgG were required for effective opsonophagocytosis due to Panzyga®'s polyclonal nature. To improve dose efficiency and minimize drug loss, the use of a breath-activated mesh nebulizer could enhance targeted delivery to overcome this challenge. The *in vitro* studies presented here lay the foundation for future investigations into this drug delivery approach.

CRediT authorship contribution statement

Rebecca Rittersberger: Writing – original draft, Visualization, Project administration, Methodology, Investigation, Formal analysis, Data curation, Conceptualization. **Caroline Covini:** Writing – review & editing, Visualization, Validation, Supervision, Project administration, Methodology, Investigation, Formal analysis, Data curation, Conceptualization. **Shruthi Kalgudde:** Writing – review & editing, Visualization, Validation, Investigation, Formal analysis, Data curation. **Pramod Kumar:** Writing – review & editing, Visualization, Validation,

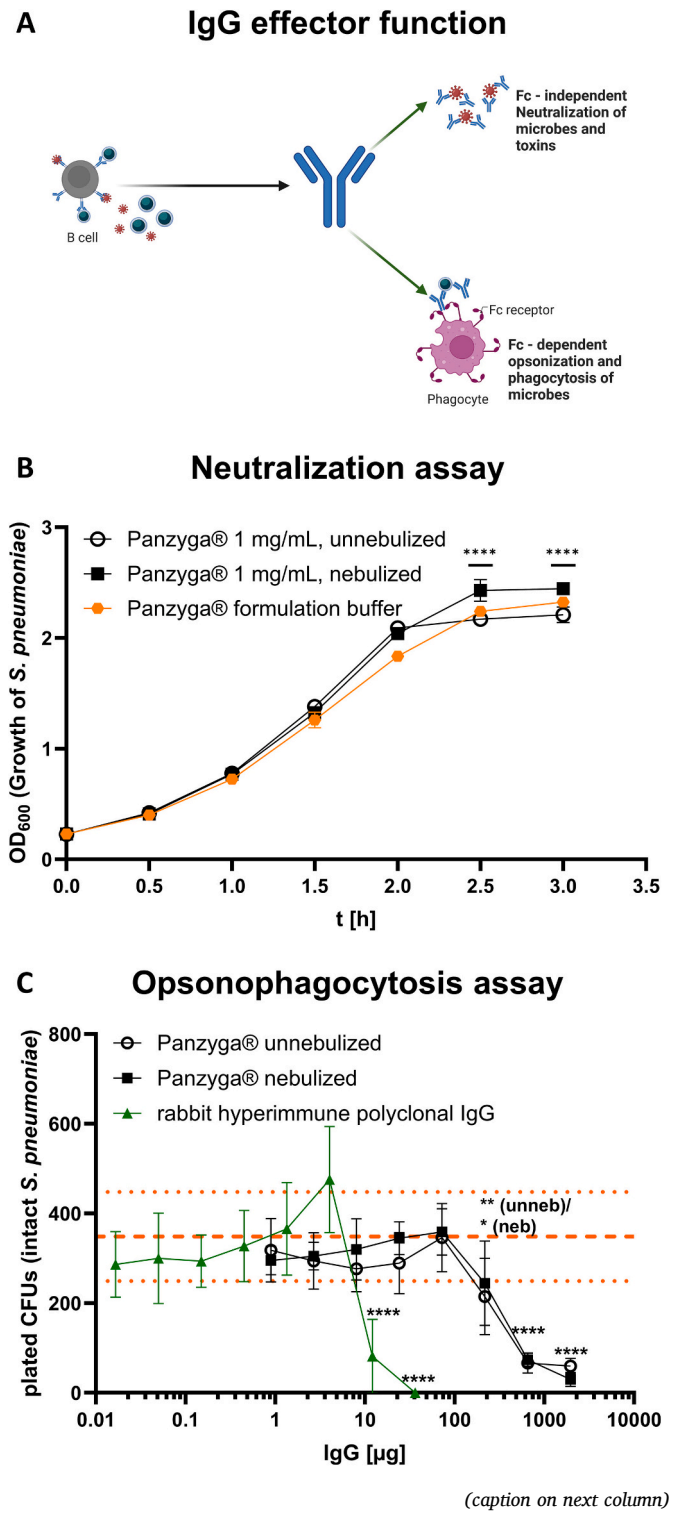

(caption on next column)

Fig. 4. Nebulized IVIg efficacy against TIGR4: growth inhibition and opsonophagocytosis of TIGR4 in murine J774.A1 macrophages. A) Fc independent neutralization *via* the Fab region and Fc dependent phagocytosis, Created under license with biorender.com. B) Neutralization/Growth inhibition assay: IVIg was added to a bacterial suspension with an OD_{600} ~ 0,2. Final IgG concentration was 1 mg/mL. As a negative control, the same volume of the formulation buffer (orange curve) was used. The OD_{600} of a 1 mL sample was measured every 30 min for 3 h. Nebulized IVIg contained 400 µg/mL PS80. N = independent experiments, $n = 15$ mL centrifugation tube per sample. $n = 2$, $N = 1$. Values are shown as mean ± SD. Two-way ANOVA; $p > 0.05$, not significant (ns); $^{*}p < 0.05$; $^{**}p < 0.01$; $^{***}p < 0.001$; $^{****}p < 0.0001$. C) Opsonophagocytosis assay: *S. pneumoniae* TIGR4 (100,000 CFU/mL) was incubated with a dilution series of nebulized IVIg or unnebulized IVIg with 400 mg/mL PS80 in OBB. Rabbit anti-pneumococcal hyperimmune IgG (green triangles) and glycine buffer served as positive and negative controls, respectively. After opsonization, bacteria were added to J774A.1 cells (MOI 400:1) for 45 min at 37 °C. Phagocytosis was stopped on ice, and viable CFUs were quantified on blood agar plates. Two-way ANOVA: $p > 0.05$, not significant (ns); $^{*}p < 0.05$; $^{**}p < 0.01$; $^{***}p < 0.001$; $^{****}p < 0.0001$. Orange dotted line presents the plated CFUs of the negative controls (OBB only and serial dilution of formulation buffer), shown as mean ± SD; $n = 6$, $N = 3$. N = independent experiments, n = wells per sample. (For interpretation of the references to colour in this figure legend, the reader is referred to the web version of this article.)

Methodology, Investigation, Formal analysis, Data curation. **Franziska Voß:** Writing – review & editing, Visualization, Validation, Methodology, Investigation, Formal analysis, Data curation. **Janik Martin:** Writing – review & editing, Visualization, Validation, Methodology, Investigation, Formal analysis. **Franziska Magdalena Deuter:** Investigation, Writing – review & editing. **Gabriel Koslowski:** Writing – review & editing, Methodology, Investigation. **Annabelle Dabbars:** Writing – review & editing, Visualization, Validation, Methodology, Investigation, Formal analysis. **Sophia Salcher:** Investigation, Writing – review & editing. **Marion Blayac:** Writing – review & editing, Visualization, Validation, Methodology, Investigation, Formal analysis, Data curation. **Jürgen Römisch:** Writing – review & editing, Supervision, Resources, Methodology, Data curation, Conceptualization. **Andrej Murányi:** Writing – review & editing, Validation, Supervision, Resources, Methodology, Investigation, Data curation, Conceptualization. **Jonas Knoch:** Writing – review & editing, Validation, Methodology. **Ali Önder Yildirim:** Writing – review & editing, Supervision, Resources, Project administration, Funding acquisition. **Thomas M. Conlon:** Writing – review & editing, Validation, Supervision, Project administration, Methodology, Investigation, Formal analysis, Data curation. **Otmar Schmid:** Writing – review & editing, Validation, Supervision, Resources, Project administration, Funding acquisition, Conceptualization. **Sven Hammerschmidt:** Writing – review & editing, Validation, Supervision, Resources, Funding acquisition, Conceptualization. **Katharina Schindowski:** Writing – original draft, Visualization, Validation, Supervision, Resources, Project administration, Funding acquisition, Conceptualization.

Funding sources

This study received funding from the European Union's Horizon 2020 research and innovation program under grant agreement No. 721098 (N2B-patch to K.S.), Deutsche Forschungsgemeinschaft

("OlfacMuc" grant No. ZI-1143/HU441 to K.S.) and Octapharma GmbH (to K.S. and O.S.). Further, the project was supported by the Bundesministerium für Bildung und Forschung (BMBF/DLR) - project Pneumofluidics – FKZ 01DP19007 (to S.H.) and BMBF-Zwanzig20 - InfectControl 2020 - project VacoME - FKZ 03ZZ0816A (to S.H.).

Declaration of competing interest

None.

Acknowledgements

The authors would like to thank Dr. René Handrick from Biberach University for excellent advisory and technical support whenever needed.

Appendix A. Supplementary data

Supplementary data to this article can be found online at https://doi.org/10.1016/j.ijpx.2025.100432.

Data availability

The data that has been used is confidential.

References

Agarkhed, M., O'Dell, C., Hsieh, M.-C., Zhang, J., Goldstein, J., Srivastava, A., 2013. Effect of polysorbate 80 concentration on thermal and photostability of a monoclonal antibody. AAPS PharmSciTech 14, 1–9. https://doi.org/10.1208/s12249-012-9878-0.

Ahmadi, M., Bryson, C.J., Cloake, E.A., Welch, K., Filipe, V., Romeijn, S., Hawe, A., Jiskoot, W., Baker, M.P., Fogg, M.H., 2015. Small amounts of sub-visible aggregates enhance the immunogenic potential of monoclonal antibody therapeutics. Pharm. Res. 32, 1383–1394. https://doi.org/10.1007/s11095-014-1541-x.

Alcorlo, M., Abdullah, M.R., Steil, L., Sotomayor, F., López-de Oro, L., de Castro, S., Velázquez, S., Kohler, T.P., Jiménez, E., Medina, A., Usón, I., Keller, L.E., Bradshaw, J.L., McDaniel, L.S., Camarasa, M.-J., Völker, U., Hammerschmidt, S., Hermoso, J.A., 2024. Molecular and structural basis of oligopeptide recognition by the Ami transporter system in pneumococci. PLoS Pathog. 20, e1011883. https://doi.org/10.1371/journal.ppat.1011883.

Antimicrobial resistance, 2024. https://www.who.int/news-room/fact-sheets/detail/antimicrobial-resistance (accessed 6 August 2024).

Ari, A., 2014. Jet, Ultrasonic, and Mesh Nebulizers: an Evaluation of Nebulizers for Better Clinical Outcomes. Eur. J. Pulmonol. 16, 1–7. https://doi.org/10.5152/ejp.2014.00087.

Arsiccio, A., Pisano, R., 2018. Surfactants as stabilizers for biopharmaceuticals: an insight into the molecular mechanisms for inhibition of protein aggregation. Eur. J. Pharmaceut. Biopharm. 128, 98–106. https://doi.org/10.1016/j.ejpb.2018.04.005.

Arunthari, V., Bruinsma, R.S., Lee, A.S., Johnson, M.M., 2012. A prospective, comparative trial of standard and breath-actuated nebulizer: efficacy, safety, and satisfaction. Respir. Care 57, 1242–1247. https://doi.org/10.4187/respcare.01450.

Auer, S., Dobson, C.M., Vendruscolo, M., 2007. Characterization of the nucleation barriers for protein aggregation and amyloid formation. HFSP J. 1, 137–146. https://doi.org/10.2976/1.2760023.

Azmin, M.N., Stuart, J.F., Calman, K.C., Florence, A.T., 1982. Effects of polysorbate 80 on the absorption and distribution of oral methotrexate (MTX) in mice. Cancer Chemother. Pharmacol. 9, 161–164. https://doi.org/10.1007/BF00257745.

Balashazy, I., Hofmann, W., Heistracher, T., 2003. Local particle deposition patterns may play a key role in the development of lung cancer. J. Appl. Physiol. (Bethesda, Md. 1985) 94, 1719–1725. https://doi.org/10.1152/japplphysiol.00527.2002.

Baranov, M.V., Kumar, M., Sacanna, S., Thutupalli, S., van den Bogaart, G., 2020. Modulation of Immune responses by Particle size and Shape. Front. Immunol. 11, 607945. https://doi.org/10.3389/fimmu.2020.607945.

Bartual, S.G., Straume, D., Stamsås, G.A., Muñoz, I.G., Alfonso, C., Martínez-Ripoll, M., Håvarstein, L.S., Hermoso, J.A., 2014. Structural basis of PcsB-mediated cell separation in Streptococcus pneumoniae. Nat. Commun. 5, 3842. https://doi.org/10.1038/ncomms4842.

Batool, S., Chokkakula, S., Song, M.-S., 2023. Influenza treatment: limitations of antiviral therapy and advantages of drug combination therapy. Microorganisms 11. https://doi.org/10.3390/microorganisms11010183.

Bebbington, C., Yarranton, G., 2008. Antibodies for the treatment of bacterial infections: current experience and future prospects. Curr. Opin. Biotechnol. 19, 613–619. https://doi.org/10.1016/j.copbio.2008.10.002.

Beck-Broichsitter, M., Oesterheld, N., Knuedeler, M.-C., Seeger, W., Schmehl, T., 2014. On the correlation of output rate and aerodynamic characteristics in vibrating-mesh-based aqueous aerosol delivery. Int. J. Pharm. 461, 34–37. https://doi.org/10.1016/j.ijpharm.2013.11.036.

Blanco-Melo, D., Nilsson-Payant, B.E., Liu, W.-C., Uhl, S., Hoagland, D., Møller, R., Jordan, T.X., Oishi, K., Panis, M., Sachs, D., Wang, T.T., Schwartz, R.E., Lim, J.K., Albrecht, R.A., tenOever, B.R., 2020. Imbalanced host response to SARS-CoV-2 drives development of COVID-19. Cell 181, 1036–1045.e9. https://doi.org/10.1016/j.cell.2020.04.026.

Blasi, F., 2004. Atypical pathogens and respiratory tract infections. Eur. Respir. J. 24, 171–181. https://doi.org/10.1183/09031936.04.00135703.

Bodier-Montagutelli, E., Mayor, A., Vecellio, L., Respaud, R., Heuzé-Vourc'h, N., 2018. Designing inhaled protein therapeutics for topical lung delivery: what are the next steps? Expert Opin. Drug Deliv. 15, 729–736. https://doi.org/10.1080/17425247.2018.1503251.

Bodier-Montagutelli, E., Respaud, R., Perret, G., Baptista, L., Duquenne, P., Heuzé-Vourc'h, N., Vecellio, L., 2020. Protein stability during nebulization: mind the collection step! Eur. J. Pharm. Biopharm. 152, 23–34. https://doi.org/10.1016/j.ejpb.2020.04.006.

Borchardt, R., Rolston, K., 2012. Respiratory tract infections: Emerging viral pathogens. JAAPA 25, 19.

Borghardt, J.M., Kloft, C., Sharma, A., 2018. Inhaled Therapy in respiratory Disease: the complex Interplay of Pulmonary Kinetic Processes. Can. Respir. J. 2018, 2732017. https://doi.org/10.1155/2018/2732017.

Borte, M., Melamed, I.R., Pulka, G., Pyringer, B., Knutsen, A.P., Ochs, H.D., Kobayashi, R. H., Kobayashi, A.L., Gupta, S., Strach, M., Smits, W., Pituch-Noworolska, A., Moy, J. N., 2017. Efficacy and safety of human intravenous immunoglobulin 10% (Panzyga®) in patients with primary immunodeficiency diseases: a two-stage, multicenter, prospective, open-label study. J. Clin. Immunol. 37, 603–612. https://doi.org/10.1007/s10875-017-0424-4.

Brennan, F.R., Morton, L.D., Spindeldreher, S., Kiessling, A., Allenspach, R., Hey, A., Muller, P.Y., Frings, W., Sims, J., 2010. Safety and immunotoxicity assessment of immunomodulatory monoclonal antibodies. mAbs 2, 233–255. https://doi.org/10.4161/mabs.2.3.11782.

Bui, V.K.H., Moon, J.-Y., Chae, M., Park, D., Lee, Y.-C., 2020. Prediction of aerosol deposition in the human respiratory tract via computational models: a review with recent updates. Atmosphere 11, 137. https://doi.org/10.3390/atmos11020137.

Cahn, D., Amosu, M., Maisel, K., Duncan, G.A., 2023. Biomaterials for intranasal and inhaled vaccine delivery. Nat. Rev. Bioeng. 1, 83–84. https://doi.org/10.1038/s44222-022-00012-6.

Cella, E., Giovanetti, M., Benedetti, F., Scarpa, F., Johnston, C., Borsetti, A., Ceccarelli, G., Azarian, T., Zella, D., Ciccozzi, M., 2023. Joining forces against Antibiotic Resistance: the one Health solution. Pathogens (Basel, Switzerland) 12. https://doi.org/10.3390/pathogens12091074.

Chang, K.H., Park, B.J., Nam, K.C., 2023. Aerosolization performance of immunoglobulin g by jet and mesh nebulizers. AAPS PharmSciTech 24, 125. https://doi.org/10.1208/s12249-023-02579-8.

Chen, W.-H., Chang, C.-M., Mutuku, J.K., Lam, S.S., Lee, W.-J., 2021. Aerosol deposition and airflow dynamics in healthy and asthmatic human airways during inhalation. J. Hazard. Mater. 416, 125856. https://doi.org/10.1016/j.jhazmat.2021.125856.

Darquenne, C., 2020. Deposition mechanisms. J. Aerosol Med. Pulm. Drug Deliv. 33, 181–185. https://doi.org/10.1089/jamp.2020.29029.cd.

Davis, J.D., Wypych, T.P., 2022. Correction: Cellular and functional heterogeneity of the airway epithelium. Mucosal Immunol. 15, 528. https://doi.org/10.1038/s41385-022-00500-3.

Dianova Int, 2025. Goat F(Ab')2 Anti-Human IgG (Fc)-RPE, MinX Bo,Ho,Ms - dianova Int. https://www.dianova.com/en/shop/109-116-098-goat-fab2-anti-human-igg-fc-rpe-minx-bohoms/ (accessed 26 August 2025).

Elm, C., Braathen, R., Bergmann, S., Frank, R., Vaerman, J.-P., Kaetzel, C.S., Chhatwal, G. S., Johansen, F.-E., Hammerschmidt, S., 2004. Ectodomains 3 and 4 of human polymeric Immunoglobulin receptor (hpIgR) mediate invasion of Streptococcus pneumoniae into the epithelium. J. Biol. Chem. 279, 6296–6304. https://doi.org/10.1074/jbc.M310528200.

European Pharmacopoeia, 2022. English: 11.0–11.2, 11th ed. Deutscher Apotheker Verlag, 11th ed. Stuttgart.

Gao, M., Mei, D., Huo, Y., Mao, S., 2019. Effect of polysorbate 80 on the intranasal absorption and brain distribution of tetramethylpyrazine phosphate in rats. Drug Deliv. Transl. Res. 9, 311–318. https://doi.org/10.1007/s13346-018-0580-y.

Garidel, P., Hoffmann, C., Blume, A., 2009. A Thermodynamic Analysis of the Binding Interaction between Polysorbate 20 and 80 with Human Serum Albumins and Immunoglobulins: A Contribution to … // a Thermodynamic Analysis of the Binding Interaction between Polysorbate 20 and 80 with Human Serum Albumins and Immunoglobulins: A Contribution to Understand Colloidal Protein Stabilisation.

Gatt, D., Martin, I., AlFouzan, R., Moraes, T.J., 2023. Prevention and Treatment strategies for respiratory Syncytial Virus (RSV). Pathogens 12. https://doi.org/10.3390/pathogens12020154.

Greeley, M.A., 2017. Immunopathology of the respiratory System. In: Parker, G.A. (Ed.), Immunopathology in Toxicology and Drug Development: Volume 2, Organ Systems. Springer International Publishing, Cham, pp. 419–453.

Grosu, A., 2022. Testing for cytotoxicity: The "well-established" EN ISO 10993-5. seleon GmbH.

Hacker, M., 2009. History of pharmacology—from antiquity to the twentieth century. In: Pharmacology. Elsevier, pp. 1–7.

Haley, P.J., 2003. Species differences in the structure and function of the immune system. Toxicology 188, 49–71. https://doi.org/10.1016/s0300-483x(03)00043-x.

Hanson, J.F., Taft, S.C., Weiss, A.A., 2006. Neutralizing antibodies and persistence of immunity following anthrax vaccination. Clin. Vaccine Immunol. CVI 13, 208–213. https://doi.org/10.1128/CVI.13.2.208-213.2006.

He, S.W.J., Voß, F., Nicolaie, M.A., Brummelman, J., van de Garde, M.D.B., Bijvank, E., Poelen, M., Wijmenga-Monsuur, A.J., Wyllie, A.L., Trzciński, K., van Beek, J.,

Rots, N.Y., Den Hartog, G., Hammerschmidt, S., van Els, C.A.C.M., 2024. Serological profiling of pneumococcal proteins reveals unique patterns of acquisition, maintenance and waning of antibodies throughout life. J. Infect. Dis. https://doi.org/10.1093/infdis/jiae216.

Henning, A., Schneider, M., Bur, M., Blank, F., Gehr, P., Lehr, C.-M., 2008. Embryonic chicken trachea as a new in vitro model for the investigation of mucociliary particle clearance in the airways. AAPS PharmSciTech 9, 521–527. https://doi.org/10.1208/s12249-008-9072-6.

Hermeling, S., Crommelin, D.J.A., Schellekens, H., Jiskoot, W., 2004. Structure-immunogenicity relationships of therapeutic proteins. Pharm. Res. 21, 897–903. https://doi.org/10.1023/b:pham.0000029275.41323.a6.

Hertel, S.P., Winter, G., Friess, W., 2015. Protein stability in pulmonary drug delivery via nebulization. Adv. Drug Deliv. Rev. 93, 79–94. https://doi.org/10.1016/j.addr.2014.10.003.

Heß, N., Waldow, F., Kohler, T.P., Rohde, M., Kreikemeyer, B., Gómez-Mejia, A., Hain, T., Schwudke, D., Vollmer, W., Hammerschmidt, S., Gisch, N., 2017. Lipoteichoic acid deficiency permits normal growth but impairs virulence of Streptococcus pneumoniae. Nat. Commun. 8, 2093. https://doi.org/10.1038/s41467-017-01720-z.

Hewitt, R.J., Lloyd, C.M., 2021. Regulation of immune responses by the airway epithelial cell landscape. Nat. Rev. Immunol. 21, 347–362. https://doi.org/10.1038/s41577-020-00477-9.

Hiemstra, P.S., McCray, P.B., Bals, R., 2015. The innate immune function of airway epithelial cells in inflammatory lung disease. Eur. Respir. J. 45, 1150–1162. https://doi.org/10.1183/09031936.00141514.

Hogan, A., Bonney, M.-A., Brien, J.-A., Karamy, R., Aslani, P., 2015. Factors affecting nebulised medicine adherence in adult patients with cystic fibrosis: a qualitative study. Int. J. Clin. Pharm. 37, 86–93. https://doi.org/10.1007/s11096-014-0043-6.

Hong, S.W., Chang, K.H., Woo, C.J., Kim, H.C., Kwak, B.S., Park, B.J., Nam, K.C., 2023. Evaluation of antibody drug delivery efficiency via nebulizer in various airway models and breathing patterns. BMC Pharmacol. Toxicol. 24, 70. https://doi.org/10.1186/s40360-023-00711-9.

Ibrahim, M., Wallace, I., Ghazvini, S., Manetz, S., Cordoba-Rodriguez, R., Patel, S.M., 2023. Protein aggregates in inhaled biologics: challenges and considerations. J. Pharm. Sci. 112, 1341–1344. https://doi.org/10.1016/j.xphs.2023.02.010.

ICRP, 1994. Human Respiratory Tract Model for Radiological Protection, 66th ed.

Jauernig, J., Mitchell, J., Berg, E., Dennis, J., Kreher, C., Lamb, P., Karlsson, M., Tservistas, M., 2008. Position paper: recommendation on the adoption of breathing patterns for infants and small children in general chapter 2.9.44. Preparations for nebulisation. Pharmeuropa Scientific Notes 2008, 31–32.

Joubert, M.K., Hokom, M., Eakin, C., Zhou, L., Deshpande, M., Baker, M.P., Goletz, T.J., Kerwin, B.A., Chirmule, N., Narhi, L.O., Jawa, V., 2012. Highly aggregated antibody therapeutics can enhance the in vitro innate and late-stage T-cell immune responses. J. Biol. Chem. 287, 25266–25279. https://doi.org/10.1074/jbc.M111.330902.

Kadioglu, A., Weiser, J.N., Paton, J.C., Andrew, P.W., 2008. The role of Streptococcus pneumoniae virulence factors in host respiratory colonization and disease. Nat. Rev. Microbiol. 6, 288–301. https://doi.org/10.1038/nrmicro1871.

Kijanka, G., Bee, J.S., Korman, S.A., Wu, Y., Roskos, L.K., Schenerman, M.A., Slütter, B., Jiskoot, W., 2018. Submicron size particles of a murine monoclonal antibody are more immunogenic than soluble oligomers or micron size particles upon subcutaneous administration in mice. J. Pharm. Sci. 107, 2847–2859. https://doi.org/10.1016/j.xphs.2018.06.029.

Kreft, M.E., Jerman, U.D., Lasič, E., Lanišnik Rižner, T., Hevir-Kene, N., Peternel, L., Kristan, K., 2015. The characterization of the human nasal epithelial cell line RPMI 2650 under different culture conditions and their optimization for an appropriate in vitro nasal model. Pharm. Res. 32, 665–679. https://doi.org/10.1007/s11095-014-1494-0.

Ladel, S., Flamm, J., Zadeh, A.S., Filzwieser, D., Walter, J.-C., Schlossbauer, P., Kinscherf, R., Lischka, K., Luksch, H., Schindowski, K., 2018. Allogenic Fc domain-facilitated uptake of igg in nasal lamina propria: friend or foe for intranasal CNS delivery? Pharmaceutics 10. https://doi.org/10.3390/pharmaceutics10030107.

Ladel, S., Schlossbauer, P., Flamm, J., Luksch, H., Mizaikoff, B., Schindowski, K., 2019. Improved in vitro model for intranasal mucosal drug delivery: primary olfactory and respiratory epithelial cells compared with the permanent nasal cell line RPMI 2650. Pharmaceutics 11. https://doi.org/10.3390/pharmaceutics11080367.

LaRocca, T.J., Katona, L.I., Thanassi, D.G., Benach, J.L., 2008. Bactericidal action of a complement-independent antibody against relapsing fever Borrelia resides in its variable region. J. Immunol. 180, 6222–6228. https://doi.org/10.4049/jimmunol.180.9.6222.

Lasagna-Reeves, C.A., Clos, A.L., Midoro-Hiriuti, T., Goldblum, R.M., Jackson, G.R., Kayed, R., 2010. Inhaled insulin forms toxic pulmonary amyloid aggregates. Endocrinology 151, 4717–4724. https://doi.org/10.1210/en.2010-0457.

Lindenberg, F., Sichel, F., Lechevrel, M., Respaud, R., Saint-Lorant, G., 2019. Evaluation of lung cell toxicity of surfactants for inhalation route. J. Toxicol. Risk Assess. 5. https://doi.org/10.23937/2572-4061.1510022.

Lu, L., Kong, W.Y., Zhang, J., Firdaus, F., Wells, J.W., Stephenson, R.J., Toth, I., Skwarczynski, M., Cruz, J.L.G., 2024. Utilizing murine dendritic cell line DC2.4 to evaluate the immunogenicity of subunit vaccines in vitro. Front. Immunol. 15, 1298721. https://doi.org/10.3389/fimmu.2024.1298721.

Marcotte, H., Hammarström, L., 2015. Passive immunization. Mucosal Immunol. 1403–1434. https://doi.org/10.1016/B978-0-12-415847-4.00071-9.

Martin, J., Rittersberger, R., Treitler, S., Kopp, P., Ibraimi, A., Koslowski, G., Sickinger, M., Dabbars, A., Schindowski, K., 2024. Characterization of a primary cellular airway model for inhalative drug delivery in comparison with the established permanent cell lines CaLu3 and RPMI 2650. In Vitro Models. https://doi.org/10.1007/s44164-024-00079-y.

Matthews, A.A., Ee, P.L.R., Ge, R., 2020. Developing inhaled protein therapeutics for lung diseases. Mol. Biomed. 1, 11. https://doi.org/10.1186/s43556-020-00014-z.

Mayor, A., Thibert, B., Huille, S., Bensaid, F., Respaud, R., Audat, H., Heuzé-Vourc'h, N., 2022. Inhaled IgG1 antibodies: the buffering system is an important driver of stability during mesh-nebulization. Eur. J. Pharmaceut. Biopharmaceut. 181, 173–182. https://doi.org/10.1016/j.ejpb.2022.11.006.

McElroy, M.C., Kirton, C., Gliddon, D., Wolff, R.K., 2013. Inhaled biopharmaceutical drug development: nonclinical considerations and case studies. Inhal. Toxicol. 25, 219–232. https://doi.org/10.3109/08958378.2013.769037.

Mersich, C., Ahrer, K., Buchacher, A., Ernegger, T., Kohla, G., Kannicht, C., Pock, K., Römisch, J., 2017. Biochemical characterization and stability of immune globulin intravenous 10% liquid (Panzyga®). Biologicals J. Int. Assoc. Biol. Standardization 45, 33–38. https://doi.org/10.1016/j.biologicals.2016.10.003.

Mettelman, R.C., Allen, E.K., Thomas, P.G., 2022. Mucosal immune responses to infection and vaccination in the respiratory tract. Immunity 55, 749–780. https://doi.org/10.1016/j.immuni.2022.04.013.

Metz, J.K., Scharnowske, L., Hans, F., Schnur, S., Knoth, K., Zimmer, H., Limberger, M., Groß, H., Lehr, C.M., Hittinger, M., 2020. Safety assessment of excipients (SAFE) for orally inhaled drug products. ALTEX 37, 275–286. https://doi.org/10.14573/altex.1910231.

Meyer, T.C., Schmidt, F., Steinke, J., Bröker, B.M., Völker, U., Michalik, S., 2020. Technical report: xMAPr - High-dynamic-range (HDR) quantification of antigen-specific antibody binding. J. Proteomics 212, 103577. https://doi.org/10.1016/j.jprot.2019.103577.

Miller, F.J., Asgharian, B., Schroeter, J.D., Price, O., 2016. Improvements and additions to the multiple path particle dosimetry model. J. Aerosol Sci. 99, 14–26. https://doi.org/10.1016/j.jaerosci.2016.01.018.

Mitchell, A.M., Mitchell, T.J., 2010. Streptococcus pneumoniae: virulence factors and variation. Clin. Microbiol. Infect. 16, 411–418. https://doi.org/10.1111/j.1469-0691.2010.03183.x.

Moussa, E.M., Panchal, J.P., Moorthy, B.S., Blum, J.S., Joubert, M.K., Narhi, L.O., Topp, E.M., 2016. Immunogenicity of therapeutic protein aggregates. J. Pharm. Sci. 105, 417–430. https://doi.org/10.1016/j.xphs.2015.11.002.

Müller-Loennies, S., Brade, L., Brade, H., 2007. Neutralizing and cross-reactive antibodies against enterobacterial lipopolysaccharide. Int. J. Med. Microbiol. IJMM 297, 321–340. https://doi.org/10.1016/j.ijmm.2007.04.002.

Nahm, M.H., Olander, J.V., Magyarlaki, M., 1997. Identification of cross-reactive antibodies with low opsonophagocytic activity for Streptococcus pneumoniae. J. Infect. Dis. 176, 698–703. https://doi.org/10.1086/514093.

Narhi, L.O., Schmit, J., Bechtold-Peters, K., Sharma, D., 2012. Classification of protein aggregates. J. Pharm. Sci. 101, 493–498. https://doi.org/10.1002/jps.22790.

Ou, C., Hang, J., Deng, Q., 2020. Particle deposition in human lung airways: effects of airflow, particle size, and mechanisms. Aerosol Air Qual. Res. 20, 2846–2858. https://doi.org/10.4209/aaqr.2020.02.0067.

Parray, H.A., Shukla, S., Perween, R., Khatri, R., Shrivastava, T., Singh, V., Murugavelu, P., Ahmed, S., Samal, S., Sharma, C., Sinha, S., Luthra, K., Kumar, R., 2021. Inhalation monoclonal antibody therapy: a new way to treat and manage respiratory infections. Appl. Microbiol. Biotechnol. 105, 6315–6332. https://doi.org/10.1007/s00253-021-11488-4.

Pilou, M., 2020. Aerosol particle deposition in the lungs: effect of breathing patterns. In: IEEE 20th International Conference on Bioinformatics and Bioengineering (BIBE) 2020, pp. 411–416. https://doi.org/10.1109/BIBE50027.2020.00073.

Podczeck, F., 1999. The Influence of Particle size distribution and Surface Roughness of carrier Particles on the in vitro Properties of Dry Powder Inhalations. Aerosol Sci. Tech. 31, 301–321. https://doi.org/10.1080/027868299304174.

Ratanji, K.D., Derrick, J.P., Dearman, R.J., Kimber, I., 2014. Immunogenicity of therapeutic proteins: influence of aggregation. J. Immunotoxicol. 11, 99–109. https://doi.org/10.3109/1547691X.2013.821564.

Röhm, M., Carle, S., Maigler, F., Flamm, J., Kramer, V., Mavoungou, C., Schmid, O., Schindowski, K., 2017. A comprehensive screening platform for aerosolizable protein formulations for intranasal and pulmonary drug delivery. Int. J. Pharm. 532, 537–546. https://doi.org/10.1016/j.ijpharm.2017.09.027.

Ruan, Y., Yao, L., Zhang, B., Zhang, S., Guo, J., 2012. Nanoparticle-mediated delivery of neurotoxin-II to the brain with intranasal administration: an effective strategy to improve antinociceptive activity of neurotoxin. Drug Dev. Ind. Pharm. 38, 123–128. https://doi.org/10.3109/03639045.2011.592533.

Sato, S., Kiyono, H., 2012. The mucosal immune system of the respiratory tract. Curr. Opin. Virol. 2, 225–232. https://doi.org/10.1016/j.coviro.2012.03.009.

Schieffelin, J.S., Costin, J.M., Nicholson, C.O., Orgeron, N.M., Fontaine, K.A., Isern, S., Michael, S.F., Robinson, J.E., 2010. Neutralizing and non-neutralizing monoclonal antibodies against dengue virus E protein derived from a naturally infected patient. Virol. J. 7, 28. https://doi.org/10.1186/1743-422X-7-28.

Schmidt, F., Meyer, T., Sundaramoorthy, N., Michalik, S., Surmann, K., Depke, M., Dhople, V., Gesell Salazar, M., Holtappels, G., Zhang, N., Bröker, B.M., Bachert, C., Völker, U., 2017. Characterization of human and Staphylococcus aureus proteins in respiratory mucosa by in vivo- and immunoproteomics. J. Proteomics 155, 31–39. https://doi.org/10.1016/j.jprot.2017.01.008.

Sécher, T., Bodier-Montagutelli, E., Parent, C., Bouvart, L., Cortes, M., Ferreira, M., MacLoughlin, R., Ilango, G., Schmid, O., Respaud, R., Heuzé-Vourc'h, N., 2022. Aggregates associated with instability of antibodies during aerosolization induce adverse immunological effects. Pharmaceutics 14. https://doi.org/10.3390/pharmaceutics14030671.

Seinen, J., Engelke, R., Abdullah, M.R., Voß, F., Michalik, S., Dhople, V.M., Dieperink, W., de Smet, A.M.G.A., Völker, U., van Dijl, J.M., Schmidt, F., Hammerschmidt, S., 2021. Sputum proteome signatures of mechanically ventilated

intensive care unit patients distinguish samples with or without anti-pneumococcal activity. mSystems 6. https://doi.org/10.1128/mSystems.00702-20.
Silva, S., Bicker, J., Falcão, A., Fortuna, A., 2023. Air-liquid interface (ALI) impact on different respiratory cell cultures. Eur. J. Pharmaceut. Biopharmaceut. 184, 62–82. https://doi.org/10.1016/j.ejpb.2023.01.013.
Singh, S.M., Bandi, S., Jones, D.N.M., Mallela, K.M.G., 2017. Effect of polysorbate 20 and polysorbate 80 on the higher-order structure of a monoclonal antibody and its fab and Fc fragments probed using 2D nuclear magnetic resonance spectroscopy. J. Pharm. Sci. 106, 3486–3498. https://doi.org/10.1016/j.xphs.2017.08.011.
Song, J.Y., Nahm, M.H., Moseley, M.A., 2013. Clinical implications of pneumococcal serotypes: invasive disease potential, clinical presentations, and antibiotic resistance. J. Korean Med. Sci. 28, 4–15. https://doi.org/10.3346/jkms.2013.28.1.4.
Steurer, L.-M., Hetzmannseder, M., Willinger, B., Starzengruber, P., Mikula-Pratschke, C., Kormann-Klement, A., Weber, M., Berger, A., Grill, A., 2022. Streptococcus pneumoniae colonization in health care professionals at a tertiary university pediatric hospital. Eur. J. Clin. Microbiol. Infect. Dis. 41, 971–976. https://doi.org/10.1007/s10096-022-04446-z.
Stützle, M., Carle, S., Engelhardt, L., Simon, U., Schafmeister, A., Mavoungou, C., Schindowski, K., 2015. Protein aerosol for intranasal nose to brain (N2B) delivery. BMC Proc. 9. https://doi.org/10.1186/1753-6561-9-S9-O11.
Tan, Y.H., Liu, M., Nolting, B., Go, J.G., Gervay-Hague, J., Liu, G., 2008. A nanoengineering approach for investigation and regulation of protein immobilization. ACS Nano 2, 2374–2384. https://doi.org/10.1021/nn800508f.
Tao, F., Han, Q., Yang, P., 2023. Interface-mediated protein aggregation. Chem. Commun. (Camb.) 59, 14093–14109. https://doi.org/10.1039/d3cc04311h.
Telikepalli, S., Shinogle, H.E., Thapa, P.S., Kim, J.H., Deshpande, M., Jawa, V., Middaugh, C.R., Narhi, L.O., Joubert, M.K., Volkin, D.B., 2015. Physical characterization and in vitro biological impact of highly aggregated antibodies separated into size-enriched populations by fluorescence-activated cell sorting. J. Pharm. Sci. 104, 1575–1591. https://doi.org/10.1002/jps.24379.
The top 10 causes of death, 2025. https://www.who.int/news-room/fact-sheets/detail/the-top-10-causes-of-death (accessed 18 February 2024).
Thorlaksen, C., Schultz, H.S., Gammelgaard, S.K., Jiskoot, W., Hatzakis, N.S., Nielsen, F. S., Solberg, H., Foderà, V., Bartholdy, C., Groenning, M., 2023. In vitro and in vivo immunogenicity assessment of protein aggregate characteristics. Int. J. Pharm. 631, 122490. https://doi.org/10.1016/j.ijpharm.2022.122490.
Tsai, C.J.Y., Loh, J.M.S., Fujihashi, K., Kiyono, H., 2023. Mucosal vaccination: onward and upward. Expert Rev. Vaccines 22, 885–899. https://doi.org/10.1080/14760584.2023.2268724.
Tschernig, T., Pabst, R., 2000. Bronchus-associated lymphoid tissue (BALT) is not present in the normal adult lung but in different diseases. Pathobiology 68, 1–8. https://doi.org/10.1159/000028109.
Verwey, C., Madhi, S.A., 2023. Review and update of active and passive immunization against respiratory syncytial virus. BioDrugs 37, 295–309. https://doi.org/10.1007/s40259-023-00596-4.
Vonarburg, C., Loetscher, M., Spycher, M.O., Kropf, A., Illi, M., Salmon, S., Roberts, S., Steinfuehrer, K., Campbell, I., Koernig, S., Bain, J., Edler, M., Baumann, U., Miescher, S., Metzger, D.W., Schaub, A., Käsermann, F., Zuercher, A.W., 2019. Topical application of nebulized human IgG, IgA and IgAM in the lungs of rats and non-human primates. Respir. Res. 20, 99. https://doi.org/10.1186/s12931-019-1057-3.
Voß, F., Kohler, T.P., Meyer, T., Abdullah, M.R., van Opzeeland, F.J., Saleh, M., Michalik, S., van Selm, S., Schmidt, F., de Jonge, M.I., Hammerschmidt, S., 2018. Intranasal vaccination with lipoproteins confers protection against pneumococcal colonisation. Front. Immunol. 9, 2405. https://doi.org/10.3389/fimmu.2018.02405.
Vultaggio, A., Matucci, A., Nencini, F., Pratesi, S., Petroni, G., Cammelli, D., Alterini, R., Rigacci, L., Romagnani, S., Maggi, E., 2012. Drug-specific Th2 cells and IgE antibodies in a patient with anaphylaxis to rituximab. Int. Arch. Allergy Immunol. 159, 321–326. https://doi.org/10.1159/000336839.
Wang, W., Singh, S.K., Li, N., Toler, M.R., King, K.R., Nema, S., 2012. Immunogenicity of protein aggregates-concerns and realities. Int. J. Pharm. 431, 1–11. https://doi.org/10.1016/j.ijpharm.2012.04.040.
Williams, B.A., Jones, C.H., Welch, V., True, J.M., 2023. Outlook of pandemic preparedness in a post-COVID-19 world. NPJ Vaccines 8, 178. https://doi.org/10.1038/s41541-023-00773-0.
Wuchner, K., Yi, L., Chery, C., Nikels, F., Junge, F., Crotts, G., Rinaldi, G., Starkey, J.A., Bechtold-Peters, K., Shuman, M., Leiss, M., Jahn, M., Garidel, P., de Ruiter, R., Richer, S.M., Cao, S., Peuker, S., Huille, S., Wang, T., Le Brun, V., 2022. Industry perspective on the use and characterization of polysorbates for biopharmaceutical products part 1: Survey report on current state and common practices for handling and control of polysorbates. J. Pharm. Sci. 111, 1280–1291. https://doi.org/10.1016/j.xphs.2022.02.009.
Yeh, H., Schum, G., 1980. Models of human lung airways and their application to inhaled particle deposition. Bull. Math. Biol. 42, 461–480. https://doi.org/10.1016/S0092-8240(80)80060-7.
Yoon, J.H., Kim, K.S., Kim, S.S., Lee, J.G., Park, I.Y., 2000. Secretory differentiation of serially passaged normal human nasal epithelial cells by retinoic acid: expression of mucin and lysozyme. Ann. Otol. Rhinol. Laryngol. 109, 594–601. https://doi.org/10.1177/000348940010900612.
Yoong, P., 2010. Enhancement of bacterial virulence by antibody neutralization of immune-activating toxins. Virulence 1, 409–413. https://doi.org/10.4161/viru.1.5.12705.
Zachari, M.A., Chondrou, P.S., Pouliliou, S.E., Mitrakas, A.G., Abatzoglou, I., Zois, C.E., Koukourakis, M.I., 2014. Evaluation of the alamarblue assay for adherent cell irradiation experiments. Dose-Response 12, 246–258. https://doi.org/10.2203/dose-response.13-024.Koukourakis.
Zangari, T., Zafar, M.A., Lees, J.A., Abruzzo, A.R., Bee, G.C.W., Weiser, J.N., 2021. Pneumococcal capsule blocks protection by immunization with conserved surface proteins. NPJ Vaccines 6, 155. https://doi.org/10.1038/s41541-021-00413-5.
Zhang, X., Li, F., Rajaraman, P.K., Comellas, A.P., Hoffman, E.A., Lin, C.-L., 2024. Investigating distributions of inhaled aerosols in the lungs of post-COVID-19 clusters through a unified imaging and modeling approach. Eur. J. Pharmaceut. Sci. 195, 106724. https://doi.org/10.1016/j.ejps.2024.106724.
Zhu, Y., Chidekel, A., Shaffer, T.H., 2010. Cultured Human Airway Epithelial Cells (Calu-3): a Model of Human respiratory Function, Structure, and Inflammatory responses. Crit. Care Res. Prac. 2010, 1–8. https://doi.org/10.1155/2010/394578.